

EXTENSION OF THE CEM2k and LAQGSM CODES TO DESCRIBE PHOTO-NUCLEAR REACTIONS

S. G. Mashnik¹, M. I. Baznat², K. K. Gudima², A. J. Sierk¹, R. E. Prael¹

¹Los Alamos National Laboratory, Los Alamos, New Mexico 87545, USA

²Institute of Applied Physics, Academy of Science of Moldova, Chişinău, Moldova

Abstract

The improved Cascade-Exciton Model (CEM) code CEM2k+GEM2 and the Los Alamos version of the Quark-Gluon String Model code LAQGSM are extended to describe photonuclear reactions. First, we incorporate into CEM2k+GEM2 new evaluations of elementary cross sections based on the latest experimental data and also make several improvements in the description of the de-excitation of nuclei remaining after the cascade stage of reactions induced by arbitrary projectiles. Next, for photonuclear reactions we include in CEM2k+GEM2 a normalization to evaluated experimental absorption cross sections based on the recent systematics by Kossov. Then, we extend our high-energy code LAQGSM by adding the photonuclear mode which was ignored in all its previous versions, and add to it the photonuclear part from our improved CEM2k+GEM2. In this work we present a short description of the photonuclear mode as incorporated into our codes, show several illustrative results, and point out some unresolved problems.

Introduction

The 2003 version [1, 2, 3] of the improved [4] Cascade-Exciton Model (CEM) [5] as realized in the code CEM2k merged [6, 7, 8] with the Generalized Evaporation Model code GEM2 by Furihata [9] and of the Los Alamos version of the Quark-Gluon String Model code LAQGSM [10] merged [6, 7, 8] with GEM2 have been recently incorporated into the transport codes MARS15 [11] and LAHET3 [12] and are planned to be incorporated in the future into the transport codes MCNPX [13] and MCNP6 [14]. Initially, neither CEM2k+GEM2 nor LAQGSM+GEM2 considered photonuclear reactions and were not able to describe such reactions, either as stand-alone codes or as event generators in transport codes. To address this problem, here we extend CEM03 (the 2003 version of CEM2k+GEM2) and LAQGSM03 (the 2003 version of LAQGSM+GEM2) codes to describe photonuclear reactions at intermediate energies (from ~ 30 MeV to ~ 1.5 GeV). We develop a model that is based on the Dubna Intranuclear Cascade (INC) Photonuclear Reaction Model (PRM) [15]–[17], uses experimental data now available in the literature, and a revision of recent systematics for the total photoabsorption cross sections by Kossov [18]. Our photonuclear reaction model still has some problems and is under further development, but even the current version allows us to describe reasonably well intermediate energy photonuclear reactions. In the following, we present a description of our model together with several illustrative results.

Dubna Photonuclear Reaction Model

The Dubna intranuclear cascade photonuclear reaction model (Dubna INC) was initially developed 35 years ago by one of us (KKG) in collaboration with Iljinov and Toneev [15] to describe photonuclear reactions at energies above the Giant Dipole Resonance (GDR) region. [At photon energies $T_\gamma = 10$ –40 MeV, the de Broglie wavelength λ is of the order of 20–5 fm, greater than the average inter-nucleonic distance in the nucleus; the photons interact with the nuclear dipole resonance as a whole, thus the INC is not applicable.] Below the pion production threshold, the Dubna INC considers absorption of photons on only “quasi-deuteron” pairs according to the Levinger model [19]:

$$\sigma_{\gamma A} = L \frac{Z(A-Z)}{A} \sigma_{\gamma d} , \quad (1)$$

where A and Z are the mass and charge numbers of the nucleus, $L \approx 10$, and $\sigma_{\gamma d}$ is the total photoabsorption cross section on deuterons as defined from experimental data.

At photon energies above the pion-production threshold, the Dubna INC considers production of one or two pions; the concrete mode of the reaction is chosen by the Monte Carlo method according to the partial cross sections (defined from available experimental data):

$$\gamma + p \rightarrow p + \pi^0 , \quad (2)$$

$$\rightarrow n + \pi^+ , \quad (3)$$

$$\rightarrow p + \pi^+ + \pi^- , \quad (4)$$

$$\rightarrow p + \pi^0 + \pi^0 , \quad (5)$$

$$\rightarrow n + \pi^+ + \pi^0 . \quad (6)$$

The cross sections of $\gamma + n$ interactions are derived from consideration of isotopic invariance, *i.e.*, it is assumed that $\sigma(\gamma + n) = \sigma(\gamma + p)$. The Compton effect on intranuclear nucleons is neglected, as its cross section is less than $\approx 2\%$ of other reaction modes (see, *e.g.*, Fig. 6.13 in Ref. [20]). The Dubna INC does not consider processes involving production of three and more pions; this limits the model applicability to photon energies $T_\gamma \lesssim 1.5$ GeV [for T_γ higher than the threshold for three-pion production, the sum of the cross sections (4)–(6) is assumed to be equal to the difference between the total inelastic $\gamma + p$ cross section and the sum of the cross sections of the two-body reactions (2)–(3)].

The kinematics of two-body reactions (2)–(3) and absorption of photons by a pair of nucleons is completely defined by a given direction of emission of one of the secondary particles. Similarly to the procedure followed for $N + N$ and $\pi + N$ interactions [21, 22], the cosine of the angle of emission of secondary particles can be represented in the c.m. system as a function of a random number ξ , distributed uniformly in the interval $[0,1]$

$$\cos \theta = 2\xi^{1/2} \left[\sum_{n=0}^N a_n \xi^n + (1 - \sum_{n=0}^N a_n) \xi^{N+1} \right] - 1 , \quad (7)$$

where $N = M = 3$,

$$a_n = \sum_{k=0}^M a_{nk} T_{\gamma}^k , \quad (8)$$

where the coefficients a_{nk} were fitted to describe the available experimental data and are published in Tabs. 1 and 2 of Ref. [17] (the corresponding coefficients for $N + N$ and $\pi + N$ interactions are published in Tab. 3 of Ref. [22] and in Tab. 72 of the monograph [16]). The distribution of the secondary particles over the azimuthal angle φ is assumed to be isotropic. After simulating the angle Θ_1 , using Eqs. (7–8), and φ_1 isotropically for the first particle of any reaction with two particles in the final state, the angles Θ_2 and φ_2 of the second particle, as well as the energies of both particles T_1 and T_2 are uniquely determined from four-momentum conservation.

The analysis of experimental data has shown that the channel (4) of two-pion photoproduction proceeds mainly through the decay of the Δ^{++} isobar listed in the last Review of Particle Physics by the Particle Data Group [23] as having the mass $M = 1232$ MeV

$$\begin{aligned} \gamma + p &\rightarrow \Delta^{++} + \pi^{-} , \\ \Delta^{++} &\rightarrow p + \pi^{+} , \end{aligned} \quad (9)$$

whereas the production cross section of other isobar components $(\frac{3}{2}, \frac{3}{2})$ are small and can be neglected. The Dubna INC uses the Lindenbaum-Sternheimer resonance model [24] to simulate the reaction (9). In accordance with this model, the mass of the isobar M is determined from the distribution

$$\frac{dW}{dM} \sim F(E, M) \sigma(M) , \quad (10)$$

where E is the total energy of the system, F is the two-body phase space of the isobar and π^{-} meson, and σ is the isobar production cross section which is assumed to be equal to the cross section for elastic $\pi^{+}p$ scattering.

The c.m. emission angle of the isobar is approximated using Eqs. (7) and (8) with the coefficients a_{nk} listed in Tab. 3 of Ref. [17]; isotropy of the decay of the isobar in its c.m. system is assumed.

In order to calculate the kinematics of the non-resonant part of the reaction (4) and two remaining three-body channels (5) and (6), the Dubna INC uses the statistical model. The total energies of the two particles (pions) in the c.m. system are determined from the distribution

$$\frac{dW}{dE_{\pi_1} dE_{\pi_2}} \sim (E - E_{\pi_1} - E_{\pi_2}) E_{\pi_1} E_{\pi_2} / E , \quad (11)$$

and that of the third particle (nucleon, N) from conservation of energy. The actual simulation of such reactions is done as follows: Using a random number ξ , we simulate in the beginning the energy of the first pion using

$$E_{\pi_1} = m_{\pi_1} + \xi(E_{\pi_1}^{max} - m_{\pi_1}),$$

where

$$E_{\pi_1}^{max} = [E^2 + m_{\pi_1}^2 - (m_{\pi_2} + m_N)^2]/2E.$$

Then, we simulate the energy of the second pion E_{π_2} according to Eq. (11) using the Monte Carlo rejection method. The energy of the nucleon is then calculated as $E_N = E - E_{\pi_1} - E_{\pi_2}$, checking that the “triangle law” for momenta

$$|p_{\pi_1} - p_{\pi_2}| \leq p_N \leq |p_{\pi_1} + p_{\pi_2}|$$

is fulfilled, otherwise this sampling is rejected and the procedure is repeated. The angles Θ and φ of the pions are sampled assuming an isotropic distribution of particles in the c.m. system,

$$\cos \Theta_{\pi_1} = 2\xi_1 - 1, \quad \cos \Theta_{\pi_2} = 2\xi_2 - 1, \quad \varphi_{\pi_1} = 2\pi\xi_3, \quad \varphi_{\pi_2} = 2\pi\xi_4,$$

and the angles of the nucleon are defined from momentum conservation, $\vec{p}_N = -(\vec{p}_{\pi_1} + \vec{p}_{\pi_2})$.

So an interaction of a photon with a nucleons inside a nucleus leads to two or three fast cascade particles. Depending on their momenta and coordinates, these particles can leave the nucleus, be absorbed, or initiate a further intranuclear cascade. All the remaining details of the Dubna INC (followed by the evaporation/fission of excited nuclei produced after the cascade stage of reactions) calculation are the same as for $N + A$ and $\pi + A$ reactions and are described in detail in the monograph [16].

The Dubna INC PRM was used successfully for many years as a stand-alone model to study different aspects of photonuclear reactions and was also incorporated without modifications into the transport codes CASCADE [25] and GEANT4 [26], and with some improvements, via CEM95 [27], CEM97 [28], and CEM2k [4], into the transport codes MARS14 [29] and MCNPX [13, 30, 31], respectively. In the middle of the 1970’s, one of the authors of the initial version of the Dubna INC PRM, Dr. A. J. Iljinov, moved from JINR, Dubna to INR, Moscow and continued to develop further the Dubna INC with his Moscow Group, which evolved into what is now known in the literature as the Moscow INC model (see, *e.g.*, [32] and references therein). The Moscow INC model was recently extended to describe photonuclear reactions at energies up to 10 GeV [33].

From CEM95 to CEM03

Photonuclear reactions were not considered in the initial version of the CEM [5]. The Dubna PRM was incorporated [34] first into the CEM95 [27] version of the CEM and used thereafter to analyze a large number of photonuclear reactions [35]. Later on, CEM95 was incorporated as an event generator into the MARS14 [29] transport code and used in some applications.

By early 1997, one of the authors of the CEM (SGM) moved from JINR, Dubna to LANL, Los Alamos, and continued to develop further with his collaborators the cascade-exciton model for LANL needs, *e.g.*, as an event generator for the Los Alamos transport code MCNPX [13] and for other applications.

New Approximations for γp Cross Sections

The first improvements in the CEM of the photonuclear mode of the Dubna INC was done in the CEM97 version [28] of the CEM. The improved cascade-exciton model in the code CEM97 differs from the older CEM95 version by incorporating new approximations for the elementary NN , πN , and γp cross sections used in the cascade, using more precise values for nuclear masses and pairing energies, employing a corrected systematics for the level-density parameters, adjusting the cross sections for pion absorption on quasi-deuteron pairs inside a nucleus, including the Pauli principle in the preequilibrium calculation, and improving the calculation of fission widths. Implementation of significant refinements

and improvements in the algorithms of many subroutines led to a decrease of the computing time by up to a factor of 6 for heavy nuclei, which is very important when performing simulations with transport codes.

Concerning specifically the photonuclear reactions, in CEM97 we developed improved approximations for the elementary γp cross sections compared with the Dubna INC PRM [15].

In the Dubna INC PRM [15] used in CEM95, the cross sections for the free γp (and for NN and πN) interactions are approximated using a special algorithm of interpolation/extrapolation through a number of picked points, mapping as well as possible the experimental data. This was done very accurately by the authors of the Dubna INC PRM [15] using all experimental data available at that time, about 35 years ago. Currently there are many more experimental data on cross section; therefore we revised the approximations of all elementary cross sections used in CEM97 [28]. We collected all published experimental data from available sources, then developed an improved algorithm for approximating cross sections and developed simple and fast approximations for elementary cross sections which fit very well presently available experimental data not only up to ~ 1.5 GeV, where the Dubna INC PRM is assumed to be used, or up to about 5 GeV, the upper recommended energy for the present version of the CEM for nucleon- and pion-induced reactions, but up to 50–100 GeV and higher, depending on availability of data. So far we have such approximations for 8 different types of $\gamma + p$ elementary cross sections and for 24 types of reactions induced by nucleons and pions. Cross sections for other types of interactions taken into account by CEM are calculated from isospin considerations using the former as input. These cross sections are used in CEM97 [28], CEM2k [4], and CEM03 [1], and were incorporated recently into the latest version of our LAQGSM [10] code, LAQGSM03 [1, 2].

We consider this part of the CEM improvement as an independently useful development, as our approximations are reliable, fast, and easy to incorporate into any transport, INC, BUU, or Glauber-type model codes. For example, our new approximations recently have been successfully incorporated by Nikolai Mokhov into the MARS14 [29] and MARS15 [11] versions of the MARS code system at Fermilab.

An example of 8 compiled $\gamma + p$ experimental cross sections together with our approximations and the old approximations from the Dubna INC PRM used in CEM95 is shown in Fig. 1. We see that these approximations describe very well all data. Although presently we have much more data than 35 years ago when the Dubna group produced their approximations used in the Dubna INC PRM [15], for a number of interaction modes like the total γp cross sections at energies below 1.2 GeV (where the initial Dubna INC PRM was assumed to be used), and for such modes as $\gamma + p \rightarrow p + \pi^0$, $\gamma + p \rightarrow n + \pi^+$, $\gamma + p \rightarrow p + \pi^+ + \pi^-$, and $\gamma + d \rightarrow n + p$, at energies not too close to their thresholds, the original approximations also agree very well with presently available data, in the energy region where the Dubna INC PRM was developed to work. This is a partial explanation of why the old Dubna INC [16] and the younger CEM95 [27] describe so well many characteristics of different nuclear reactions. On the other hand, for some elementary cross sections like $\gamma + p \rightarrow p + 2\pi^0$ and $\gamma + p \rightarrow n + \pi^+ + \pi^0$, the old approximations differ significantly from the present data, demonstrating the need for a better description of all modes of photonuclear reactions. (Similar results were obtained in CEM97 [28] for hadron-hadron cross section approximations.)

The CEM97 code with these cross sections and the other mentioned improvements was incorporated by Gallmeier [30] into the MCNPX transport code [13], allowing MCNPX to consider for the first time interaction of intermediate-energy photons with thick targets of practically arbitrary geometry.

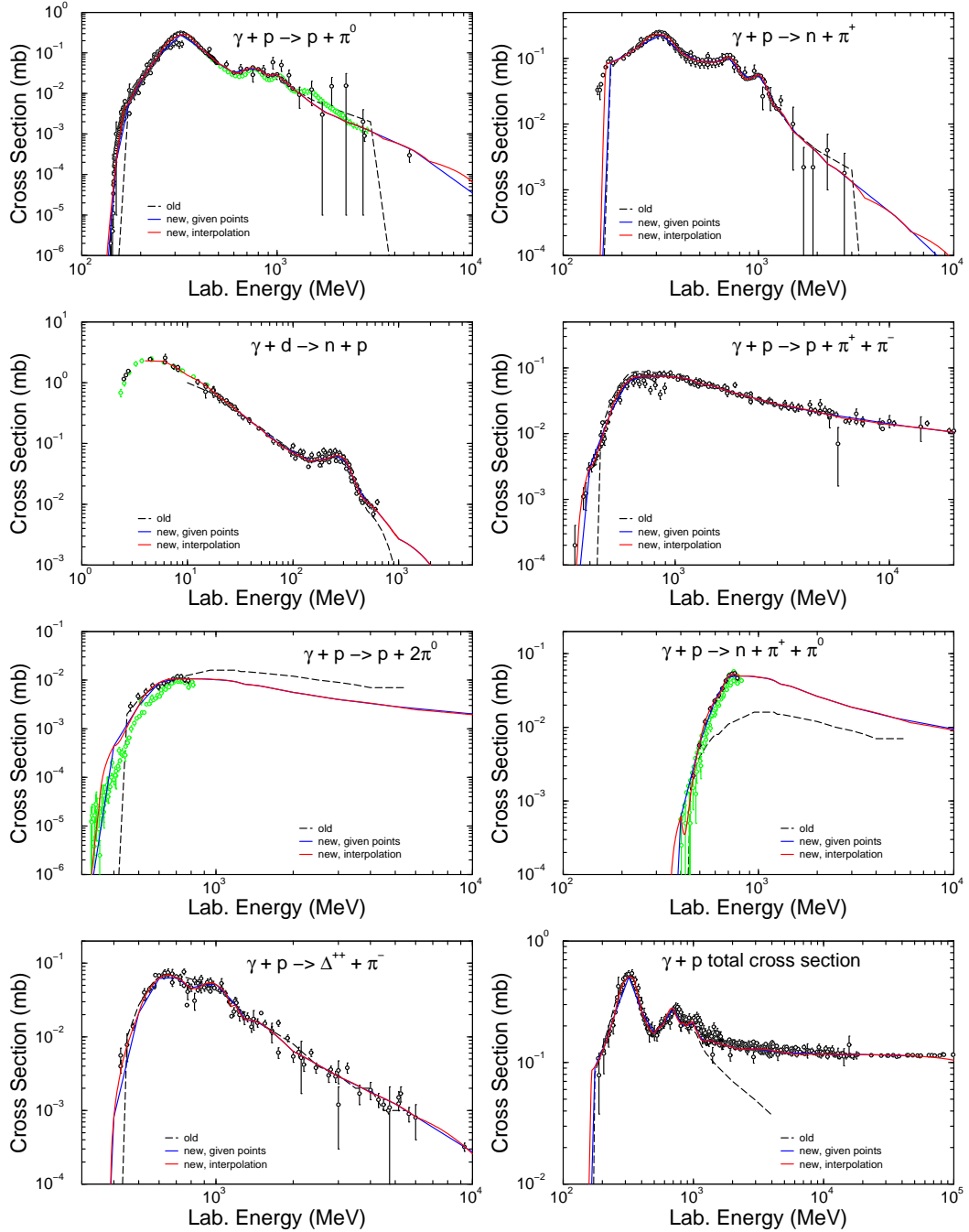


Figure 1: Comparison of eight experimental total $\gamma + p(d)$ cross sections with the old approximations used in the Dubna INC PRM and with our approximations incorporated into the CEM03 and LAQGSM03 codes. The red curve gives the code results using parabolic interpolation, while the blue solid curve uses linear interpolation between our tabulated points. Where no blue curve is visible, it is coincident with the red curve. Experimental data (black and green circles) are compiled from: $\gamma + p \rightarrow p + \pi^0$: [36]–[45]; $\gamma + p \rightarrow n + \pi^+$: [36]–[39], [46]–[51]; $\gamma + d \rightarrow n + p$: [23, 37], [52]–[72]; $\gamma + p \rightarrow p + \pi^+ + \pi^-$: [37, 42], [73]–[76]; $\gamma + p \rightarrow p + 2\pi^0$: [73], [77]–[79]; $\gamma + p \rightarrow n + \pi^+ + \pi^0$: [73, 80, 81]; $\gamma + p \rightarrow \Delta^{++} + \pi^-$: [37]; $\gamma + p$ total cross sections: [23, 37, 51, 52], respectively. The green circles show recent experimental data that became available to us after we completed our fit; Although these recent data agree reasonably well with our approximations, a refitting would slightly improve the agreement.

The CEM2k [4] version of CEM is a “new generation” of the CEM following CEM97 [28]. Its development was partially motivated by the availability of some new, very precise and useful experimental data obtained recently at GSI in Darmstadt, Germany, where a large number of measurements have been performed using inverse kinematics for interactions of ^{56}Fe , ^{197}Au , ^{208}Pb , and ^{238}U at 1500, 1000, 800, 750, 500, and 300 MeV/nucleon with liquid ^1H . These measurements provide a large set of cross sections for production of practically all possible isotopes from such reactions in a “pure” form, *i.e.*, individual cross sections from a specific given bombarding isotope (or target isotope, when considering reactions in the usual kinematics, $p + A$). Such cross sections are much easier to compare to models than the “camouflaged” data from γ -spectrometry measurements. In addition, many reactions where a beam of light, medium, or heavy ions with energy near to or below 1 GeV/nucleon interact with different nuclei, from the lightest, d , to the heaviest, ^{208}Pb were measured recently at GSI. References on these measurements and many tabulated experimental cross sections may be found on the Web page of Prof. K.-H. Schmidt [82].

(We have analyzed with CEM2k and LAQGSM all measurements done at GSI of which we are aware, both for proton-nucleus and nucleus-nucleus interactions; some examples of our results compared with the GSI data and calculations by other available models may be found in [3] and references therein.)

During the development of the CEM2k version of CEM and of LAQGSM, we concentrated mainly on proton-nucleus and nucleus-nucleus reactions and tried to improve the general description of different types of nuclear reactions by our models, without focussing specifically on photonuclear reactions. The main difference of CEM2k from its precursor CEM97 is in the criterion for when to move from the intranuclear-cascade stage of a reaction to its preequilibrium stage, and when to move from the latter to the evaporation/fission slow stage of the reaction. In short, CEM2k has a longer cascade stage, less preequilibrium emission, and a longer evaporation stage with a higher excitation energy, as compared to CEM97 and CEM95. Besides these changes to CEM97, we also made in CEM2k a number of other improvements and refinements, such as imposing momentum-energy conservation for each simulated event (the Monte Carlo algorithm previously used in CEM provides momentum-energy conservation only statistically, on the average, but not exactly for each simulated event); using real binding energies for nucleons at the cascade stage of a reaction instead of the approximation of a constant separation energy of 7 MeV used in previous versions of the CEM; using reduced masses of particles in the calculation of their emission widths instead of using the approximation of no recoil used in previous versions; and coalescence of complex particles from fast cascade nucleons already outside the nucleus. On the whole, CEM2k describes better than CEM97 and CEM95 many nuclear reactions, including the ones induced by photons. CEM2k was incorporated by Gallmeier into MCNPX to replace CEM97, and this version of MCNPX was extended by him to describe photonuclear reactions also in the GDR region [31] (as a stand-alone code, CEM2k was developed to describe photonuclear reactions only at energies above the GDR region).

We have focused on the improved description of specifically the photonuclear reactions when developing our latest version of CEM, CEM03 [1]. Although CEM97 contained new approximations and algorithms to better describe the integrated elementary NN , πN , and γN cross sections as mentioned above, the double differential distributions of secondary particles from such interactions were simulated by CEM2k and all its precursors using the old Dubna INC approximations (7)–(11) for γp reactions (and similar relations, for NN and πN collisions). These were obtained by Gudima *et al.* [15, 21, 22] 36 years ago, using the measurements available at that time. In CEM03, for NN and πN collisions, we addressed this problem by developing new approximations similar to (7)–(11) and by using recent systematics by other authors, based on experimental data available today (see details on

NN and πN reactions in [1]). In the case of γp reactions (2) and (3), we chose another way: Instead of fitting the parameters a_n from Eq. (7) at different E_γ we found data (see, *e.g.*, Figs. 2 and 3) and finding the energy dependence of parameters a_{nk} in Eq. (8) using the values obtained for a_n , we took advantage of the event generator for γp and γn reactions from the Moscow INC [33] kindly sent us by Dr. Igor Pshenichnov. That event generator includes a data file with smooth approximations through presently available experimental data at 50 different gamma energies from 117.65 to 6054 MeV (in the system where the p or n interacting with γ is at rest) for the c.m. angular distributions $d\sigma/d\Omega$ of secondary particles as functions of Θ tabulated for values of Θ from 0 to 180 deg., with the step $\Delta\Theta = 10$ deg., for 60 different channels of γp and γn reactions considered by the Moscow INC (see details in [33]). We use part of that data file with data for reactions (2) and (3), and have written an algorithm to simulate unambiguously $d\sigma/d\Omega$ and to choose the corresponding value of Θ for any E_γ , using a single random number ξ uniformly distributed in the interval $[0,1]$. This is straightforward due to the fact that the function $\xi(\cos\Theta)$

$$\xi(\cos\Theta) = \frac{\int_{-1}^{\cos\Theta} d\sigma/d\Omega d\cos\Theta}{\int_{-1}^1 d\sigma/d\Omega d\cos\Theta}$$

is a smooth monotonic function increasing from 0 to 1 as $\cos\Theta$ varies from -1 to 1. Naturally, when E_γ differs from the values tabulated in the data file, we perform first the needed interpolation in energy. We use this procedure to describe in CEM03 angular distributions of secondary particles from reactions (2) and (3), as well as for isotopically symmetric reactions $\gamma + n \rightarrow n + \pi^0$ and $\gamma + n \rightarrow p + \pi^-$.

Examples of eight angular distributions of π^0 from $\gamma p \rightarrow \pi^0 p$ and of π^+ from $\gamma p \rightarrow \pi^+ n$ as functions of $\Theta_{c.m.s}^\pi$ are presented in Figs. 2 and 3. We see that the approximations developed in CEM03 (solid histograms) agree much better with the available experimental data than the old Dubna INC approximations (7)–(8) used in all precursors of CEM03 (dashed histograms).

New Approximations for $\gamma + A$ Absorption Cross Sections

CEM03 (and its predecessors) does not consider absorption of low energy photons in the GDR region and takes into account photoproduction on free nucleons of only two pions. This restricts its applicability to the range $30 \text{ MeV} \lesssim E_\gamma \lesssim 1.5 \text{ GeV}$, which is not convenient when it is used as an event generator in a transport code.

To extend the applicability of CEM03 (and LAQGSM03) into the GDR region, it is necessary to omit the intranuclear cascade (INC) and to consider such reactions as starting with the preequilibrium model. The INC used by CEM03 as the first stage of arbitrary reactions is a semiclassical model that does not consider any collective degrees of freedom of a nucleus, including the GDR; in addition, the energy of a γ in the GDR region is too low to justify the use of any INC. In our approach, it is possible to deal with this limitation as was done 30 years ago [122], using the Modified Exciton Model (MEM) [123, 124] used in the initial version of CEM [5] and 25 years later [125], using an improved version of the MEM contained in the CEM95 [27] code. We plan to extend CEM03 to describe photonuclear reactions in the GDR region in the near future, but this requires a large amount of tedious work: 1) to make sure that we use the most reliable parameters of the GDR for all nuclei, 2) to define an optimal transition from the current three-stage (INC, preequilibrium, and evaporation/fission) description of reactions to a two-stage approach needed in the GDR region, and 3) to test the extended model against available experimental data.

To describe properly with CEM03 and LAQGSM03 photonuclear reactions above $E_\gamma \sim 1.5 \text{ GeV}$, it is necessary to take into account production of more than two pions in γN collisions, as well as to consider production of resonances heavier than $\Delta(1232)$, as has been done, *i.e.*, in the Moscow INC [33]. We plan to extend CEM03 and LAQGSM03 to higher E_γ in subsequent versions.

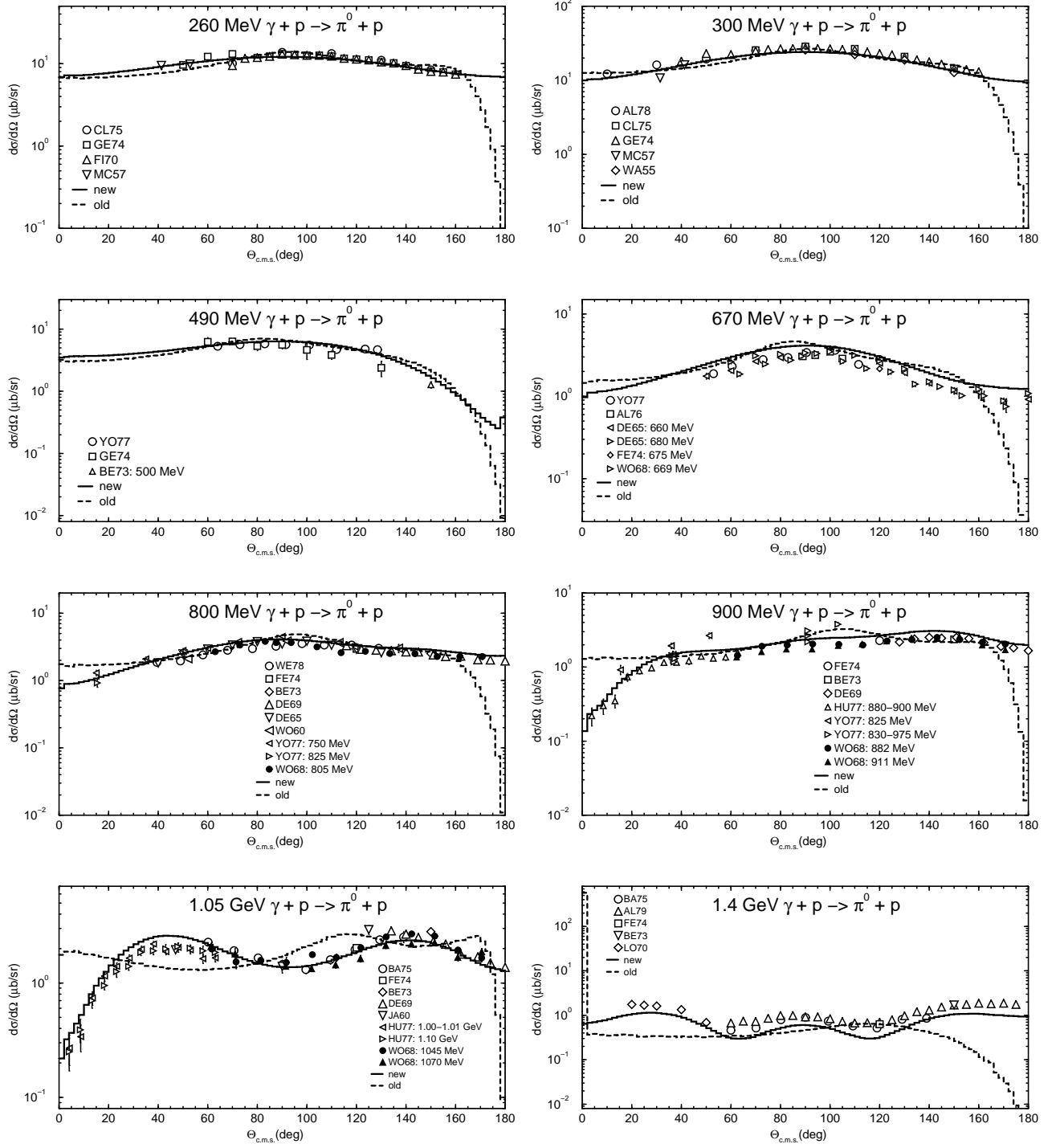


Figure 2: Example of eight angular distributions of π^0 from $\gamma p \rightarrow \pi^0 p$ as functions of $\Theta_{c.m.s.}^\pi$ at photon energies from 260 MeV to 1.4 GeV. The dashed lines show the old approximations used in the Dubna INC PRM while the solid lines are our new approximations incorporated into the CEM03 and LAQGSM03 codes. Experimental data are shown by symbols and are from: CL75 [83], GE74 [84], FI70 [85], MC57 [86], AL78 [87], WA55 [88], YO77 [89], BE73 [90], AL76 [91], DE65 [92], FE74 [93], WO68 [94], WE78 [95], DE69 [96], WO60 [97], HU77 [98], BA75 [99], JA60 [100], AL79 [101], and LO70 [102]; tabulated values are available at: <http://www-spires.dur.ac.uk/hepdata/reac2.html>.

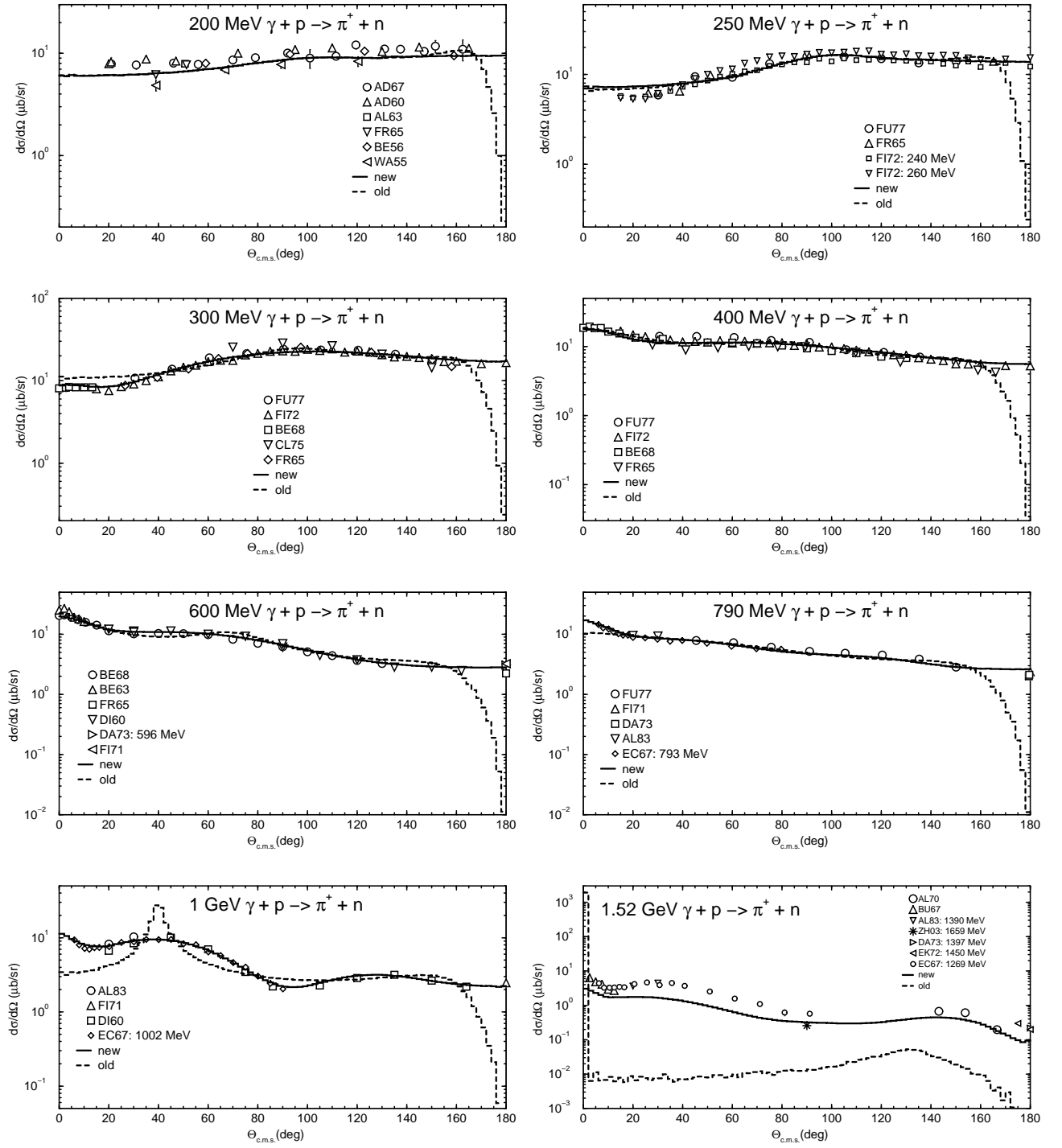


Figure 3: Example of eight angular distributions of π^+ from $\gamma p \rightarrow \pi^+ n$ as functions of $\Theta_{c.m.s}^\pi$ at photon energies from 200 MeV to 1.52 GeV. The dashed lines show the old approximations used in the Dubna INC PRM while the solid lines are our new approximations incorporated into the CEM03 and LAQGSM03 codes. Experimental data are shown by symbols and are from: AD67 [103], AS60 [104], AL63 [105], FR65 [106], BE56 [107], WA55 [108], FU77 [109], FI72 [110], BE68 [111], CL75 [83], BE63 [112], DI60 [113], DA73 [114], FI71 [115], AL83 [116], EC67 [117], AL70 [118], BU67 [119], ZH03 [120], and EK72 [121]; tabulated values are available at: <http://www-spires.dur.ac.uk/hepdata/reac2.html>.

In the meantime, for applications it is possible to get quite reasonable results for spectra of emitted nucleons and complex particles and for the nuclide production cross sections with our present CEM03 model for photonuclear reactions both in the GDR region and at $E_\gamma \gtrsim 1.5$ GeV, by employing a correct total photoabsorption cross section. Indeed, CEM03 starts a reaction in the GDR region with a cascade and since the γ energy is below the pion-production threshold, the only available reaction channel is to absorb such photons on a quasideuteron pair of nucleons, generating two “cascade” nucleons inside the nucleus. As the energy of these nucleons is low, ~ 10 MeV, these nucleons are “absorbed” by the nucleus generating two excited nucleons (excitons) and two holes, then CEM03 would proceed with this process as a preequilibrium reaction followed by evaporation/fission. All the real calculation of such reactions would be done with only the preequilibrium and evaporation models and the INC would serve only to provide the number of excitons, as an input to the MEM. At the end of the calculation, the total photoabsorption (reaction) cross section is needed to normalize the results. CEM03 (and most other INC models) calculates the total reaction cross section, σ_{in} , by the Monte Carlo method using the geometrical cross section, σ_{geom} , and the number of inelastic, N_{in} , and elastic, N_{el} , simulated events, namely: $\sigma_{in} = \sigma_{geom} N_{in} / (N_{in} + N_{el})$. This approach provides a good agreement with available data for reactions induced by nucleons, pions, and photons at incident energies above about 100 MeV, but is not reliable at energies below 100 MeV (see, *e.g.*, Figs. 3 and 4 and Ref. [7]).

To address this problem for photonuclear reactions, we have written a FORTRAN routine GABS based on the recent approximation by Kossov [18], that provides reliable photoabsorption cross sections on arbitrary targets at all energies from the hadron production threshold to about 40 TeV. We have added GABS to CEM03 to normalize our photonuclear results to this systematics rather than to σ_{in} calculated by the Monte Carlo method, as we have done previously. (As a rule, we use LAQGSM03 only at energies above several GeV, where CEM03 becomes already not reliable; at such high energies, LAQGSM03 describes quite well σ_{in} and does not require renormalization of its results to any systematics; therefore we do not incorporate GABS into LAQGSM03.)

The Kossov approximation [18] of the energy dependence of photonuclear cross sections is subdivided into three main regions: the GDR region, the nucleon resonance region, and the high-energy region. Its functional form is also subdivided into three groups depending on the mass number of the target: the $\sigma_{\gamma p}$ cross section, the cross section for γd reactions, and the $\sigma_{\gamma A}$ cross section for $A > 2$.

The Kossov approximation [18] of $\sigma_{\gamma p}$ (in mb) as a function of the photon energy E (in MeV) is of the following form:

$$\sigma_{\gamma p} = f_r \cdot (r_\Delta + r_H) + g_4 + g_8 + f_p \cdot h_p^{(p)}, \quad (12)$$

where

$$f_r = (1 + e^{25 \cdot (5.24 - z)})^{-1}, \quad (13)$$

$$r_\Delta = \frac{0.55}{1 + \frac{(z - u_\Delta(1))^2}{w_\Delta(1)}}, \quad (14)$$

$$u_\Delta(A) = 5.82 - \frac{0.07}{1 + 0.003 \cdot A^2}, \quad (15)$$

$$w_\Delta(A) = 0.056 + \ln(A) \cdot (0.03 - 0.001 \cdot \ln(A)), \quad (16)$$

$$r_H = \frac{0.223}{1 + \frac{(z - 6.57)^2}{w_H(1)}}, \quad (17)$$

$$w_H(A) = 0.045 + 0.04 \cdot (\ln(A))^{\frac{3}{2}}, \quad (18)$$

$$g_4 = \frac{e^{4 \cdot (6.27 - z)}}{1 + e^{12 \cdot (7.25 - z)}}, \quad (19)$$

$$g_8 = \frac{e^{8 \cdot (6.66 - z)}}{1 + e^{24 \cdot (6.9 - z)}} , \quad (20)$$

$$f_p = (1 + e^{4 \cdot (7 - z)})^{-1} , \quad (21)$$

$$h_p^{(p)} = 0.0375 \cdot (z - 16.5) + 1.07 \cdot e^{-0.11 \cdot z} , \quad (22)$$

and $z = \ln(E)$.

For γd reactions, the Kossov approximation is as follows:

$$\sigma_{\gamma d} = f_r \cdot (r_\Delta + r_H) + g_1 + g_2 + g_4 + g_8 + s_p(2) f_p h_p(2) , \quad (23)$$

where

$$f_r = (1 + e^{25 \cdot (\tau_r(2) - z)})^{-1} , \quad (24)$$

$$\tau_r(A) = 5.13 - 0.00075 \cdot A , \quad (25)$$

$$r_\Delta = \frac{0.88}{1 + \frac{(z - u_\Delta(2))^2}{w_\Delta(2)}} , \quad (26)$$

$$r_H = \frac{0.348}{1 + \frac{(z - 6.575)^2}{w_H(2)}} , \quad (27)$$

$$g_1 = \frac{e^{1 \cdot (1.86 - z)}}{1 + e^{3 \cdot (1.2 - z)}} , \quad (28)$$

$$g_2 = \frac{e^{2 \cdot (2.11 - z)}}{1 + e^{6 \cdot (1.5 - z)}} , \quad (29)$$

$$g_4 = \frac{e^{4 \cdot (6.2 - z)}}{1 + e^{12 \cdot (7.1 - z)}} , \quad (30)$$

$$g_8 = \frac{e^{8 \cdot (6.62 - z)}}{1 + e^{24 \cdot (6.91 - z)}} , \quad (31)$$

$$s_p(A) = A \cdot (1 - 0.072 \cdot \ln(A)) , \quad (32)$$

$$h_p(A) = 0.0375 \cdot (z - 16.5) + s_h(A) \cdot e^{-0.11 \cdot z} , \quad (33)$$

$$s_h(A) = 1.0663 - 0.0023 \cdot \ln(A) . \quad (34)$$

For γA reactions, when $A > 2$, the Kossov approximation is similar to Eq. (23) but has a different functional form, therefore it is more convenient to write it as follows:

$$\sigma_{\gamma A} = \sigma_{GDR} + f_r(r_\Delta + r_H) + s_p(A) f_p h_p(A) , \quad (35)$$

where the “global” approximation for the photoabsorption cross section in the GDR region can be written as

$$\sigma_{GDR} = g_1 + g_2 + g_4 + g_8 , \quad (36)$$

$$g_i = \frac{e^{i \cdot (\rho_i - z)}}{1 + e^{3i \cdot (\tau_i - z)}} , \quad (37)$$

$$\rho_1 = \frac{3.2 + 0.75 \cdot \ln(A)}{1 + (2/A)^4} , \quad (38)$$

$$\tau_1 = \frac{6.6 - 0.5 \cdot \ln(A)}{1 + (2/A)^4} , \quad (39)$$

$$\rho_2 = \frac{4.0 + 0.125 \cdot \ln(A)}{1 + (2/A)^4} , \quad (40)$$

$$\tau_2 = \frac{3.4}{1 + (2/A)^4} , \quad (41)$$

$$\rho_4 = 3.8 + 0.05 \cdot \ln(A) , \quad (42)$$

$$\tau_4 = 3.8 - 0.25 \cdot \ln(A) , \quad (43)$$

$$\rho_8 = 3.65 - 0.05 \cdot \ln(A) , \quad (44)$$

$$\tau_8 = 3.5 - 0.16 \cdot \ln(A) . \quad (45)$$

We note that Eq. (45) was misprinted in the original publication by Kossov [18] (it corresponds to Eq. (41) in [18]) where a “+” sign occurs instead of a “−” sign. The misprinted formula does not reproduce the cross sections presented in [18], whereas the corrected version does.

Figs. 4 and 5 show examples of twelve photoabsorption cross sections on several light, medium, and heavy nuclei. In these figures, we compare predictions of the Kossov systematics as implemented in the routine GABS with available experimental data and with the LANL, KAERI, and the BOFOD(MOD) (IPPE/Obninsk and CDFE/Moscow) evaluations from the IAEA Photonuclear Data Library [126], as well as with calculations by two older versions of CEM, namely, the CEM95 photonuclear code version [34] and CEM2k as modified by Gallmeier [31] for MCNPX.

The Kossov systematics describe well the experimental photoabsorption cross sections and agree with the LANL, KAERI, and the BOFOD evaluations, especially for heavy targets. For ^{12}C , ^{27}Al , and ^{63}Cu (and several other nuclei we tested but did not include in Figs. 4 and 5) the agreement in the GDR region is not so good. This is because we use here the “global” approximation given by Eqs. (36)–(45) to calculate the photoabsorption cross section in the GDR region for all nuclei. It is known from the literature that the GDR of light nuclei differ significantly from the ones of heavy nuclei, and should be addressed carefully for each light nucleus separately. In fact, Kossov [18] had fitted the parameters of the light nuclei separately and his results shown in Figs. 2–7 of Ref. [18] for the light nuclei agree better with the data than the “global” systematics shown here does. Unfortunately, Kossov did not publish in [18] the parametrization of the GDR he found for every light nucleus (some details of this are listed in the recent *GEANT4 Physics Reference Manual* [156] and in [157], but only for some light nuclei, and those details differ from what is published in [18]). To fill this gap, we hope to determine ourselves a parameterization of the GDR photoabsorption on light nuclei using all available experimental data.

Illustrative Results

In this Section, we present several illustrative results from CEM03 and LAQGSM03 extended to describe photonuclear reactions. We start with photofission cross sections, which we have compiled from the literature and have analyzed with both CEM03 and LAQGSM03. Fig. 6 shows a comparison of such data for ^{197}Au , ^{208}Pb , ^{209}Bi , ^{232}Th , ^{233}U , ^{235}U , ^{238}U , and ^{237}Np to results of CEM03, as well as to several earlier versions, namely, the photonuclear versions of CEM95 [34], CEM98 [158], CEM2k+GEM2 [8], and the modified version of CEM2k incorporated into MCNPX by Gallmeier [31]. The CEM03 results agree well with the experimental fission cross sections, and better than the results of the earlier models. Using in CEM03 (and CEM2k+GEM2) the Kossov approximation for the total photoabsorption cross sections allows us to describe the fission cross section not only for photon energies from ~ 30 MeV to ~ 1.5 GeV, where the model is expected to be reliable, but also outside this region, in the whole range from 10 MeV to 5 GeV.

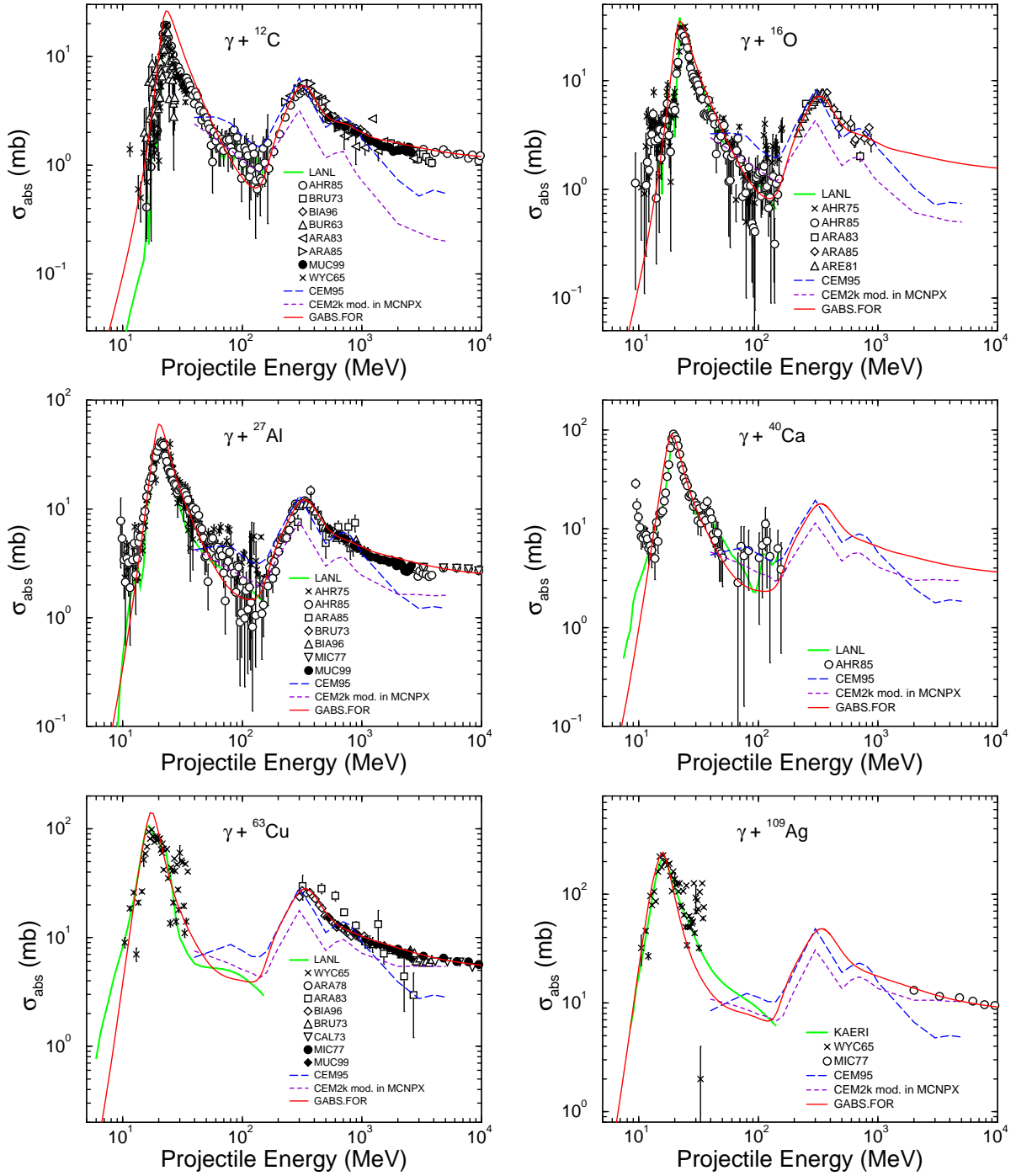


Figure 4: Examples of total photoabsorption cross sections for ^{12}C , ^{16}O , ^{27}Al , ^{40}Ca , ^{63}Cu , and ^{109}Ag as functions of photon energy. The red lines marked as “GABS.FOR” are from our subroutine written to reproduce Kossov’s [18] systematics, as described in the text. The green line marked as “LANL” (or “KAERI”, for ^{109}Ag) show the evaluations by LANL (or KAERI, for ^{109}Ag) from the IAEA Photonuclear Data Library [126]. Results from the photonuclear version of CEM95 [34] and from CEM2k as modified for MCNPX by Gallmeier [31] are shown by the blue and brown dashed lines, respectively. Experimental data (symbols) are from: AHR85 [127], BRU73 [128], BIA96 [129], BUR63 [130], ARA83 [131], ARA85 [132], MUC99 [133], WYC65 [134], AHR75 [135], ARE81 [136], MIC77 [137], ARA78 [138], and CAL73 [139].

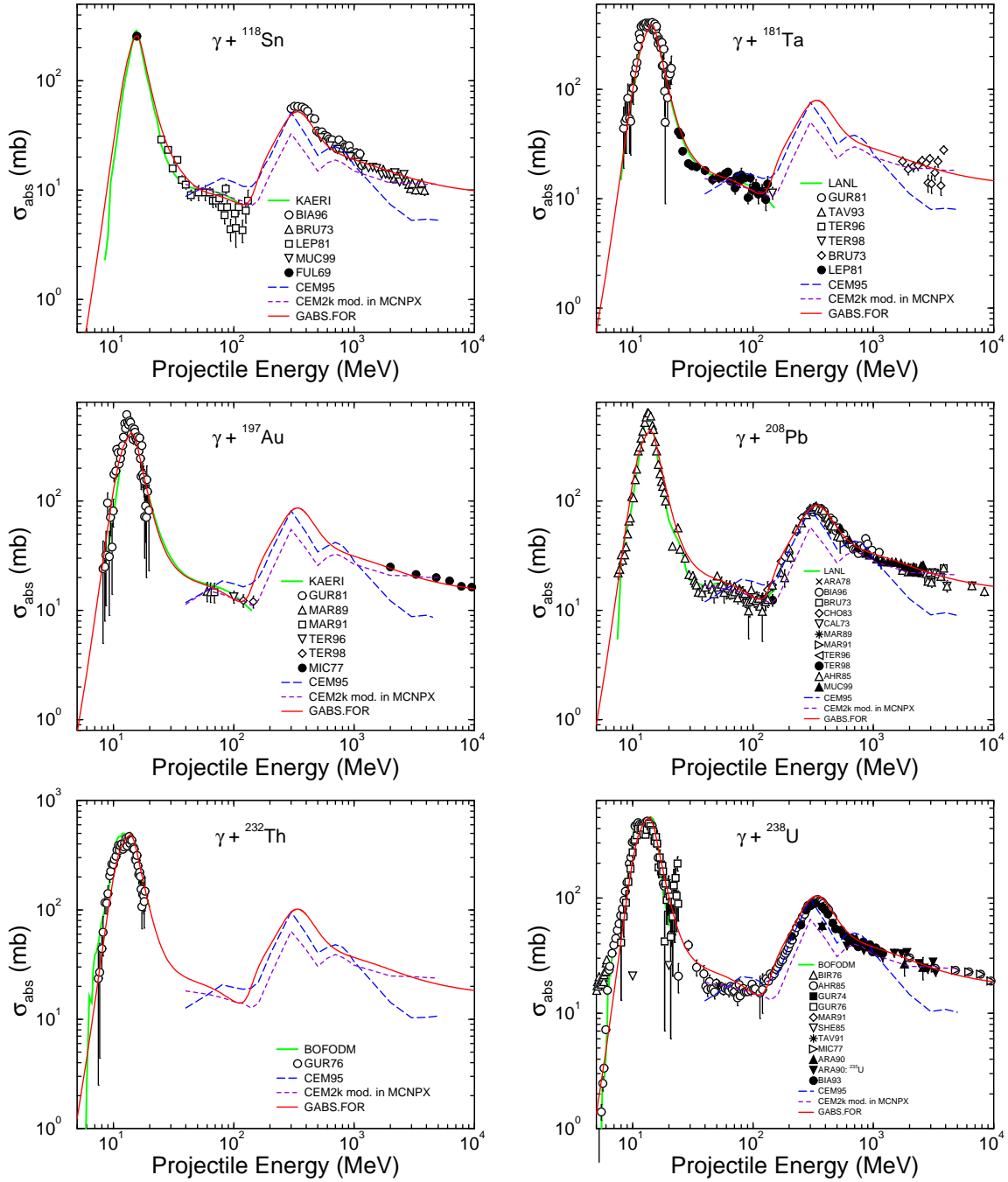


Figure 5: Examples of total photoabsorption cross sections for ^{118}Sn , ^{181}Ta , ^{197}Au , ^{208}Pb , ^{232}Th , and ^{238}U as functions of photon energy. The red lines marked as “GABS.FOR” are results by our subroutine written to reproduce Kossov’s [18] systematics, as described in the text. The green line marked as “LANL”, “KAERI”, or “BOFODM” show the evaluations by LANL, KAERI, or by a collaboration between IPPE/Obninsk and CDFE/Moscow (the BOFOD(MOD) Library) from the IAEA Photonuclear Data Library [126]. Results from the photonuclear version of CEM95 [34] and from CEM2k as modified for MCNPX by Gallmeier [31] are shown by the blue and brown dashed lines, respectively. Experimental data (symbols) are from: BIA96 [129], BRU73 [128], LEP81 [140], MUC99 [133], FUL69 [141], GUR81 [142], TAV93 [143], TER96 [144], TER98 [145], MAR89 [146], MAR91 [147], MIC77 [137], ARA78 [138], CHO83 [148], CAL73 [139], AHR85 [127], GUR76 [149], BIR76 [150], GUR74 [151], SHE85 [152], TAV91 [153], ARA90 [154], and BIA93 [155].

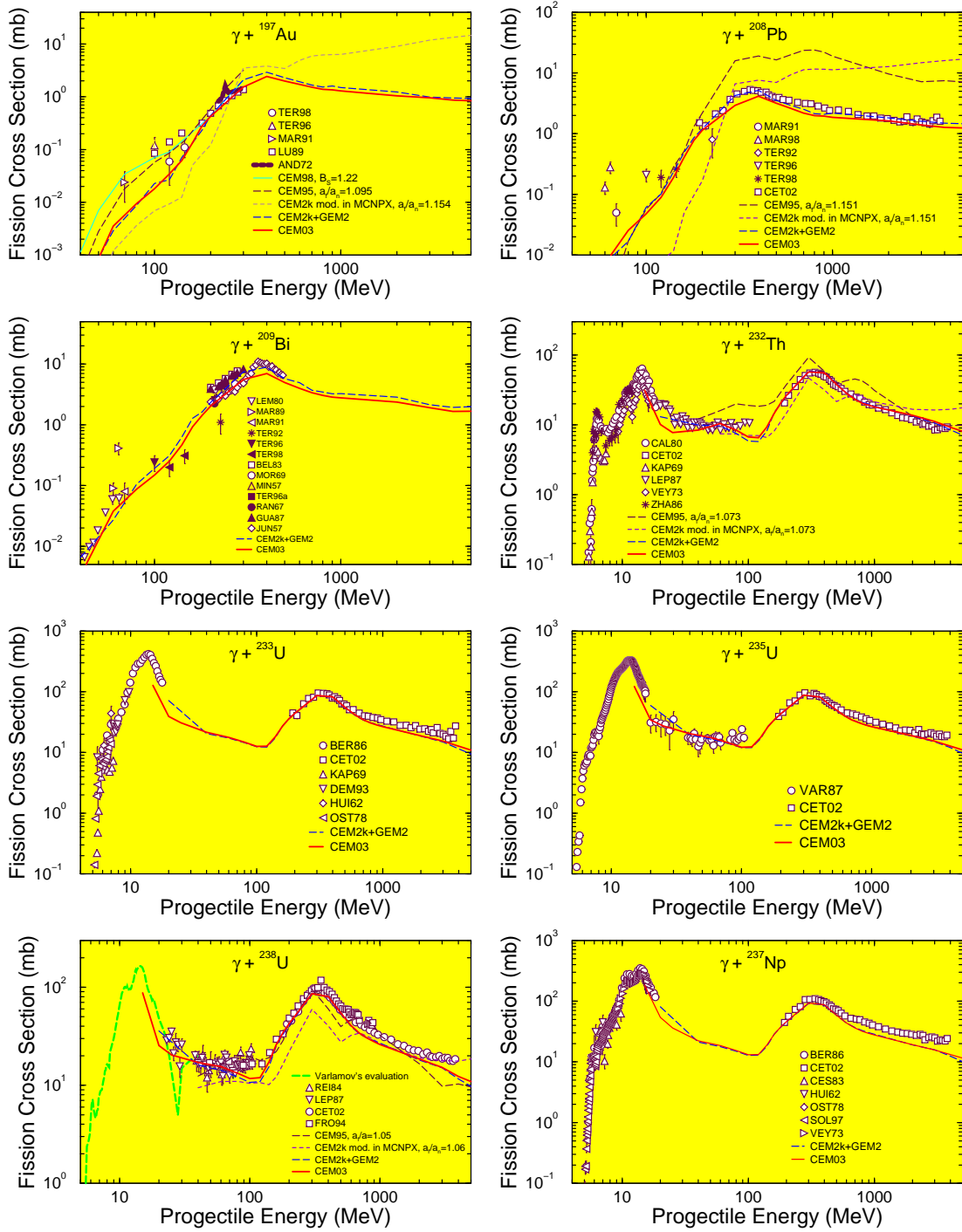


Figure 6: Comparison of calculated photofission cross sections on ${}^{197}\text{Au}$, ${}^{208}\text{Pb}$, ${}^{209}\text{Bi}$, ${}^{232}\text{Th}$, ${}^{233}\text{U}$, ${}^{235}\text{U}$, ${}^{238}\text{U}$, and ${}^{237}\text{Np}$ with experimental data (symbols), results by previous versions of CEM (see details and references in the text), and the statistical evaluation by Varlamov *et al.* from independent measurements [159], as indicated. Experimental data are from: TER98 [145], TER96 [144], MAR89 [146], MAR91 [147], LU89 [160], AND72 [161], TER92 [162], CET02 [163], LEM80 [164], BEL83 [165], MOR69 [166], MIN57 [167], TER96a [168], RAN67 [169], GUA87 [170], JUN57 [171], CAL80 [172], KAP69 [173], LEP87 [174], VEY73 [175], ZHA86 [176], BER86 [177], DEM93 [178], HUI62 [179], OST78 [180], VAR87 [159], REI84 [181], FRO94 [182], CES83 [183], OST78 [180], and SOL97 [184].

This is an example of getting reasonably good results outside the region where the model is justified, as discussed in the previous Section. Results of LAQGSM03 for these fission cross sections practically coincide with the ones by CEM03 above the GDR region, as the calculation of fission cross sections in CEM03 and LAQGSM03 were developed to be (see details in [8]), but are significantly lower than the data in the GDR region, as LAQGSM03 does not use the Kossow approximation and so should not be applied in the GDR region. Results of CEM95, CEM98, and CEM2k are also below the data in the GDR region, for the same reason.

We note that all the CEM03 and LAQGSM03 results shown in Fig. 6 and in the following figures are obtained using default and fixed values of all parameters, without fitting anything. We only specify in the inputs to CEM03 (and CEM2k+GEM2) and LAQGSM03 the energy of the incident photons and A and Z of the target, then calculate. CEM95, CEM98, and CEM2k use a parameter whose value affects drastically the calculated fission cross sections, just as in many similar statistical models: This is the ratio of the level density parameters used in the fission and evaporation channels, a_f/a_n (or, B_s , in the case of CEM98, see details in [158]). The fission cross sections calculated by any code employing the statistical evaporation and fission models depend so much on a_f/a_n that by fitting this ratio it is possible to get a good agreement with the measured data (but not to predict unmeasured fission cross sections) with any reasonable values for the fission barriers, nuclide masses, pairing energies, and deformations, for any particular measured reaction. This is why some published papers that analyze fission cross sections or even pretend to obtain “experimental fission barriers” without addressing the question of a_f/a_n are of low significance. In our CEM95, CEM98, and CEM2k calculations, we use the default options for nuclear masses, pairing energies, and fission barriers (the “recommended” options, in the case of CEM95, where several options are available in its input; see details in [27]), but we still need to define (more exactly, to fit) the values of a_f/a_n (or, B_s , in the case of CEM98): These values are listed on our plots in Fig. 6. Naturally, CEM2k+GEM2, CEM03, and LAQGSM03 also had in the beginning the problem of a_f/a_n , but this problem was solved in [8] by fitting these parameters for proton-induced fission cross sections for all targets for which we found data, at all incident energies, and by their extrapolation/interpolation for unmeasured targets. The fitted values are fixed and are used in all our further CEM03 and LAQGSM03 calculations without subsequent variation; this allows us not only to describe well most of the measured data but also to predict reasonably well unmeasured fission cross sections. The fitting procedure [8] was done so that both CEM03 (and CEM2k+GEM2) and LAQGSM03 describe as well as possible all available proton-induced measured fission cross sections; this is why the fission cross sections calculated by CEM03 practically coincide with the ones obtained by LAQGSM03 and with the experimental data.

We note that both CEM03 and LAQGSM03 assume that the reactions occur generally in three stages (see *e.g.* [185]). The first stage is the IntraNuclear Cascade (INC), in which primary particles can be re-scattered and produce secondary particles several times prior to absorption by, or escape from the nucleus. When the cascade stage of a reaction is completed, both our codes use the coalescence model described in [186] to “create” high-energy d , t , ^3He , and ^4He by final-state interactions among emitted cascade nucleons, already outside of the target. The emission of the cascade particles determines the particle-hole configuration, Z , A , and the excitation energy that is the starting point for the second, pre-equilibrium stage of the reaction. The subsequent relaxation of the nuclear excitation is treated in terms of the modified exciton model of pre-equilibrium decay followed by the equilibrium evaporation/fission stage of the reaction. Generally, all four components may contribute to experimentally measured particle spectra and distributions. But if the residual nuclei after the INC have atomic numbers with $A \leq 12$, both CEM03 and LAQGSM03 use the Fermi break-up model described in [10] to calculate their further disintegration instead of using the pre-equilibrium and evaporation models. The Fermi break-up is much faster than, and gives results very similar to, the continuation of the more detailed models to much lighter nuclei.

Figs. 7 and 8 show two examples of proton spectra calculated by CEM03 and LAQGSM03 compared with experimental data for the reactions 300 MeV $\gamma + \text{Cu}$ [187] and 198 MeV $\gamma + \text{C}$ [188], respectively. Both codes describe quite well the proton spectra in the case of copper, but less well for carbon.

Fig. 9 shows examples of π^+ angular distributions from 213 MeV γ 's interacting with Pb, Sn, Ca, and C targets. One can see that the π^+ angular distributions calculated by CEM03 agree reasonably well with the experimental data [189] for C, Ca, and Sn targets, but underestimate by a factor of 2 to 3 the Pb data. We do not have a good understanding of this disagreement. One possible explanation of this would be if CEM03 absorbs too strongly the low-energy pions produced in γp collisions inside the target. The heavier the target the bigger would be this effect, therefore we may see it with Pb but not observe it for C, Ca, and Sn targets. There also could be problems with the experimental data for Pb. As noted in [189], there is a systematic error in these data associated with the correction for the electron contamination in the yield for the forward detectors with $Z \geq 20$ targets. For instance, because of the magnitude of this background, no experimental cross sections are reported for the Pb target at 51° [189].

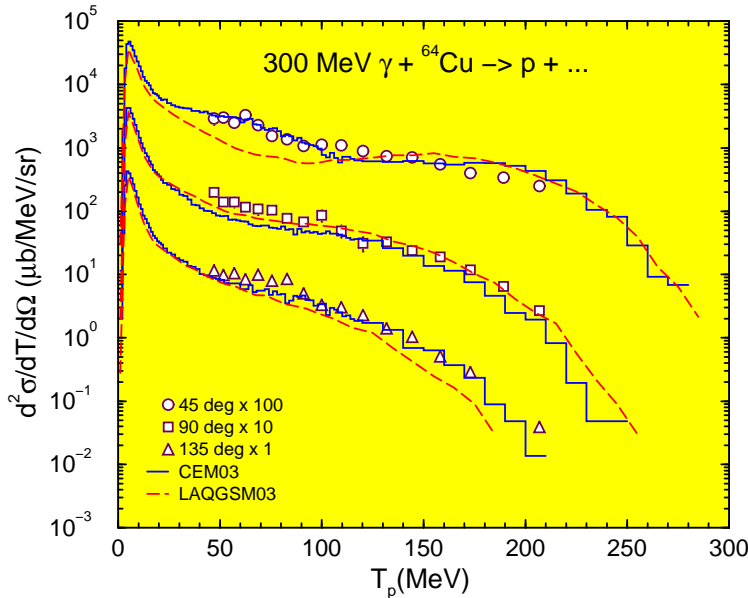


Figure 7: Proton spectra at 45° , 90° , and 135° from the reaction 300 MeV $\gamma + \text{Cu}$. Symbols are experimental data from [187], histograms and dashed lines are results of CEM03 and LAQGSM03, respectively.

We now consider another type of photonuclear reaction, induced by bremsstrahlung photons. In contrast to reactions induced by monoenergetic photons of a given energy E , the bremsstrahlung beam is produced by monoenergetic electrons and has a spectrum of photon energies E of the form $N(E, E_0) \sim 1/E$ [190], from 0 to E_0 , where the end-point energy E_0 is the maximum energy of photons produced by the given electron beam. In addition, all experimental characteristics for reactions induced by bremsstrahlung photons are normalized per “equivalent quanta”, Q , defined as:

$$Q = \frac{1}{E_0} \int_0^{E_0} E \cdot N(E, E_0) dE \bigg/ \int_0^{E_0} N(E, E_0) dE. \quad (46)$$

As discussed above, since CEM03 and LAQGSM03 do not describe properly photonuclear reactions in the GDR region, we can calculate with our codes bremsstrahlung reactions while limiting ourselves to photon energies only above the GDR region.

This means we need to simulate in our calculations the energies of the bremsstrahlung photons according to their spectrum $N(E, E_0) \sim 1/E$ up to E_0 not from 0, but from a value E_{min} , above the

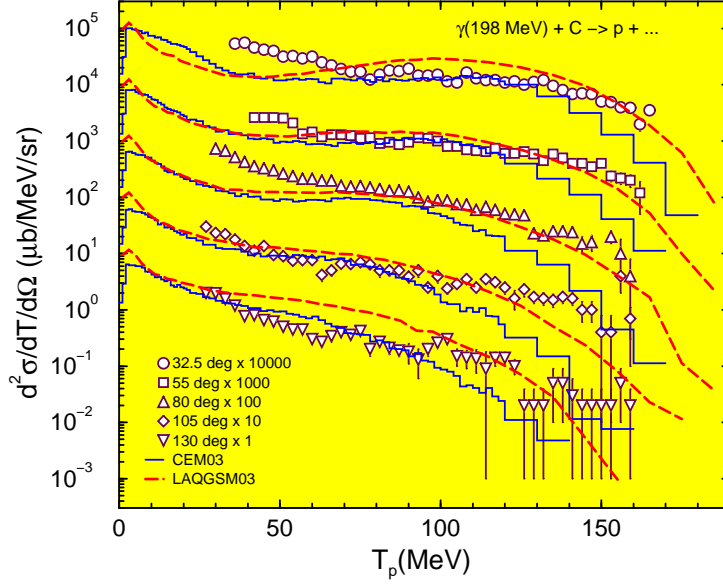


Figure 8: Proton spectra at 32.5°, 55°, 80°, 105°, and 130° from the reaction 198 MeV $\gamma + C$. Symbols are experimental data from [188], histograms and dashed lines are results from CEM03 and LAQGSM03, respectively.

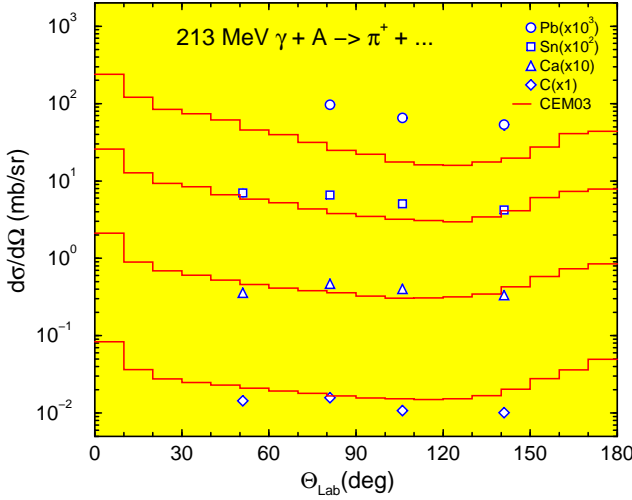


Figure 9: Energy-integrated angular distributions $d\sigma/d\Omega$ of π^+ emitted from 213 MeV γ interactions with Pb, Sn, Ca, and C. Symbols show experimental data by Fissum *et al.* [189] while histograms show CEM03 results.

GDR region, and in calculating the number of equivalent quanta Q , we need to use E_{min} for the lower limits of the integrals in Eq. (46) instead of 0. This is easy to do in our Monte Carlo calculations. After simulation of N_{in} numbers of interactions of bremsstrahlung gammas of energy E_i with a nucleus, the number of equivalent quanta Q will be:

$$Q = \frac{1}{N_{in}E_0} \sum_i E_i = \frac{\langle E \rangle}{E_0}, \quad (47)$$

where the mean energy of the bremsstrahlung photons $\langle E \rangle$ is equal to

$$\langle E \rangle = \frac{\int_{E_{min}}^{E_0} E \cdot N(E, E_0) dE}{\int_{E_{min}}^{E_0} N(E, E_0) dE} = \frac{\sum_i E_i}{N_{in}}, \quad (48)$$

and $E_{min} \leq E_i \leq E_0$. In the present paper, we use $E_{min} = 30$ MeV for all the reactions we discuss. The total inelastic (photoabsorption) cross section σ_{in} in the case of bremsstrahlung photons is calculated

as following:

$$\sigma_{in} = \frac{\int_{E_{min}}^{E_0} \sigma_{in}^{\gamma}(E) \cdot N(E, E_0) dE}{\int_{E_{min}}^{E_0} N(E, E_0) dE} = \frac{\sum_i \sigma_{in}^{\gamma}(E_i)}{N_{in}}, \quad (49)$$

where $\sigma_{in}^{\gamma}(E_i)$ is the photoabsorption cross section by a nucleus of a photon with $E_{\gamma} = E_i$, simulated in a particular Monte Carlo event i .

By using here for E_{min} a value of 30 MeV instead of 0, we will miss in our results the products from interaction of γ with energies below 30 MeV, like the cross sections for (γ, n) , $(\gamma, 2n)$, and, to a certain degree, (γ, np) , but this limitation does not affect at all description of products in the deep spallation, fission (for preactinides), and fragmentation regions, as well as the pion photoproduction and spectra of nucleons and complex particles at energies above the evaporation region.

Figs. 10 and 11 present examples of proton and π^+ spectra from bremsstrahlung interaction with carbon at $E_0 = 1050$ and 305 MeV, respectively. One can see that CEM03 describes well both proton and pion measured spectra and agrees with the data better than the direct knockout model [192] and quasideuteron calculations [193] do.

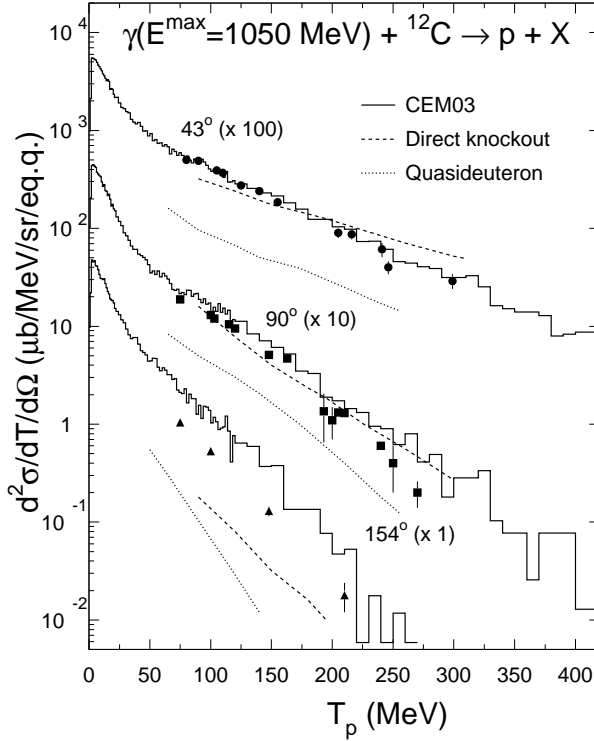


Figure 10: Comparison of measured [191] differential cross section for proton photoproduction on carbon at 43° , 90° , and 154° by bremsstrahlung photons with $E^{max}(\equiv E_0) = 1.05$ GeV (symbols) with CEM03 calculations (histograms), and predictions by the direct knockout model [192] (dashed lines) and a quasideuteron calculation [193] (dotted lines), respectively. The experimental data and results by the direct knockout and quasideuteron models were taken from Fig. 5 of Ref. [192].

Since the 1980's, a large number of radiochemical measurements of bremsstrahlung-induced reactions have been performed in Japan by the group of Prof. Koh Sakamoto (see the recent reviews [195, 196] and references therein). Thousands of useful product cross sections were measured by this group on target nuclei from ^7Li to ^{209}Bi at bremsstrahlung end-point energies E_0 from 30 MeV to 1.2 GeV, including photopion reactions, fragmentation and fission of preactinides, deep spallation reactions, and recoil studies (mean kinetic energy and the forward/backward (F/B) ratios of products). The authors of these measurements have analyzed most of their data with the PICA code by Tony Gabriel *et al.* [197, 198], with its improved version PICA95 [199, 200], as well as with its latest version, PICA3, which merged [201] with the mentioned above GEM evaporation-fission code by Shiori

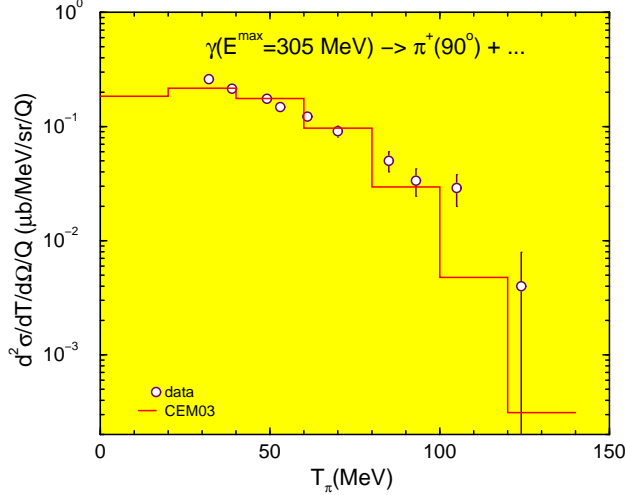


Figure 11: Comparison of measured [194] differential cross section for π^+ photoproduction on carbon at 90° by bremsstrahlung photons with $E^{max}(\equiv E_0) = 305$ MeV (circles) with CEM03 calculations (histogram).

Furihata [9], *i.e.*, PICA3/GEM.

Recently, this group provided us with numerical values of some of their measured reactions and we have calculated them with CEM03. Fig. 12 shows an example of the comparison of CEM03 results with data for bremsstrahlung-induced fission cross sections of ^{197}Au [202] and ^{209}Bi [203], compared as well with other available experimental data for Au [169, 171], [204]–[209] and for Bi [166, 169, 171, 207, 208], [210]–[212], and with results by PICA3/GEM [201] from [203]. There is a very good agreement of the CEM03 results with the experimental data in the whole interval of E_0 measured, from the threshold to the highest measured energy.

Fig. 13 presents experimental data [202, 203], [213]–[216] and calculations by PICA3/GEM [201] and by CEM03 for the isotopic yields of products produced by bremsstrahlung reactions on ^{197}Au and ^{209}Bi at $E_0 = 1$ GeV. For convenience, all the isotopes produced in these reactions were divided into four groups, namely: 1) spallation products produced by sequential emission of several nucleons, positive pions, and complex particles during the INC, followed by preequilibrium and evaporation processes; 2) intermediate-mass nuclides produced via fission of excited compound nuclei; 3) light fragments emitted either via evaporation or by “fragmentation” (Fermi break-up model, in the case of our present results), and 4) “photopion” products produced in $(\gamma, \pi^- xn)$ and $(\gamma, 2\pi^- xn)$ reactions, where the charge of the products is higher than that of the initial target. One can see that CEM03 describes the yields of products in all these groups and agrees with the experimental data and results by PICA3/GEM. CEM03 does not describe well the spallation products very near the target, that are produced via (γ, xn) reactions, because it does not consider photons with energies in the GDR region ($E_{min} = 30$ MeV), as discussed above. We note that the CEM03 and PICA3/GEM results shown in the figure report A -distributions of the yield of all products, *i.e.*, sums over Z of yields of all isotopes with a given mass number A , while the experimental data obtained by the radiochemical method generally represent results for only several isotopes (sometimes, for only a single isotope) that contribute to the corresponding data point. That is, this comparison is only qualitative but not quantitative and provides us only an approximate picture of the agreement between the calculations and measured data. Radiochemical measurements present the total yield for a given A only for cases when cumulative cross sections that include contributions from all precursors of all possible Z to the given measured yield; therefore, in general theoretical calculations of A -distribution of yields should be higher than many experimental radiochemical data points. A much better, quantitative analysis would be to compare only the measured cross sections, isotope-by-isotope, as we did earlier for proton-induced reactions (see, *e.g.*, [3, 217] and references therein). We plan to perform such an analysis of isotopic yields from photonuclear reactions in the future.

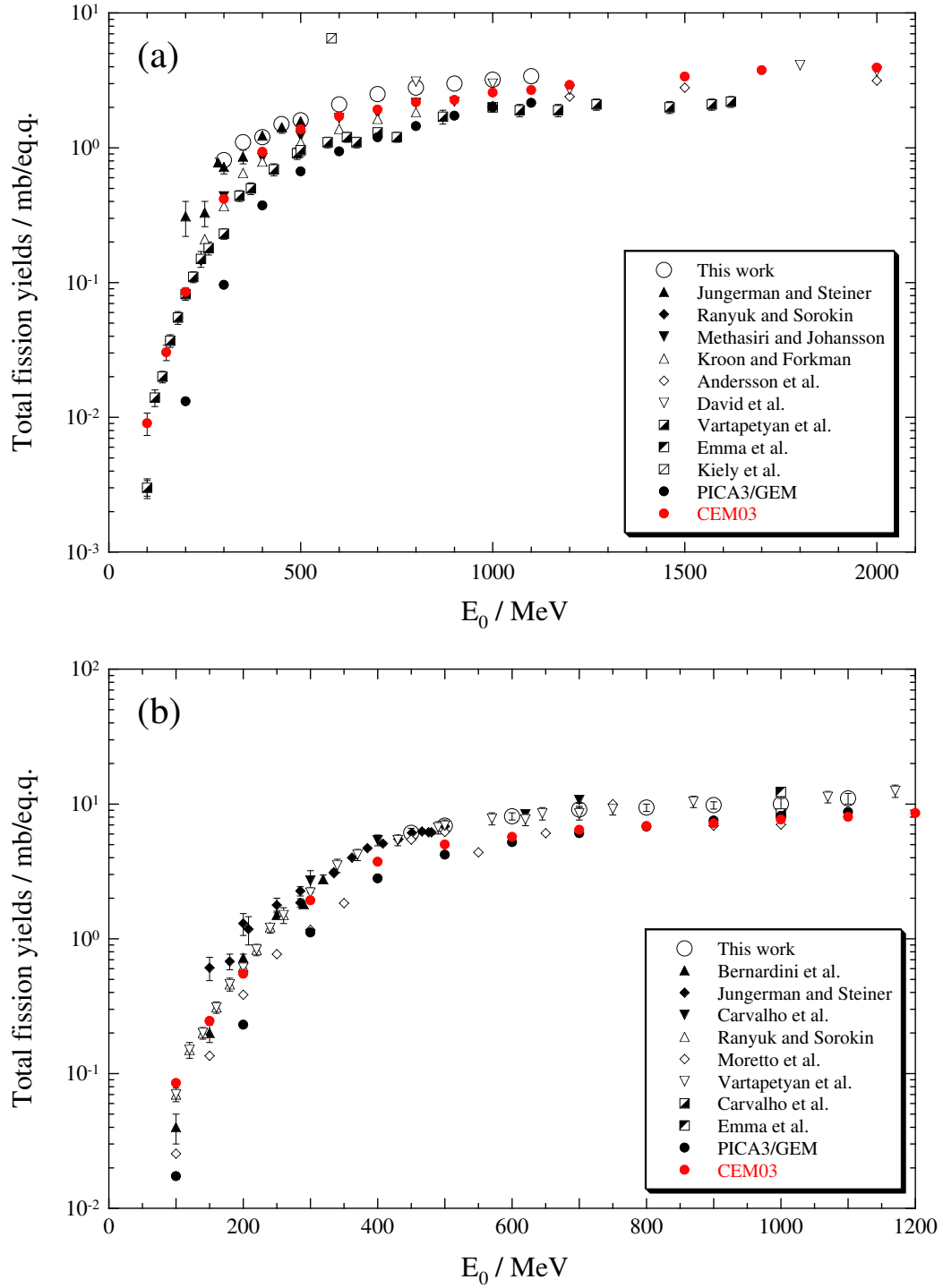


Figure 12: Bremsstrahlung-induced fission cross sections of ^{197}Au (a) and ^{209}Bi (b) as functions of the end-point energy E_0 . The experimental data for Au indicated in the insert of the figure as “This work” are from [202]; other experimental data on Au are from [169, 171], [204]–[209], as indicated. The data for Bi indicated as “This work” are from [203] and other data for Bi are from [166, 169, 171, 207, 208], [210]–[212], as indicated. The PICA3/GEM [201] results are from [203]; our present CEM03 results are shown as red circles. We thank Dr. Hiromitsu Haba for making this figure for us by adding our CEM03 results to Fig. 19 of the review [195].

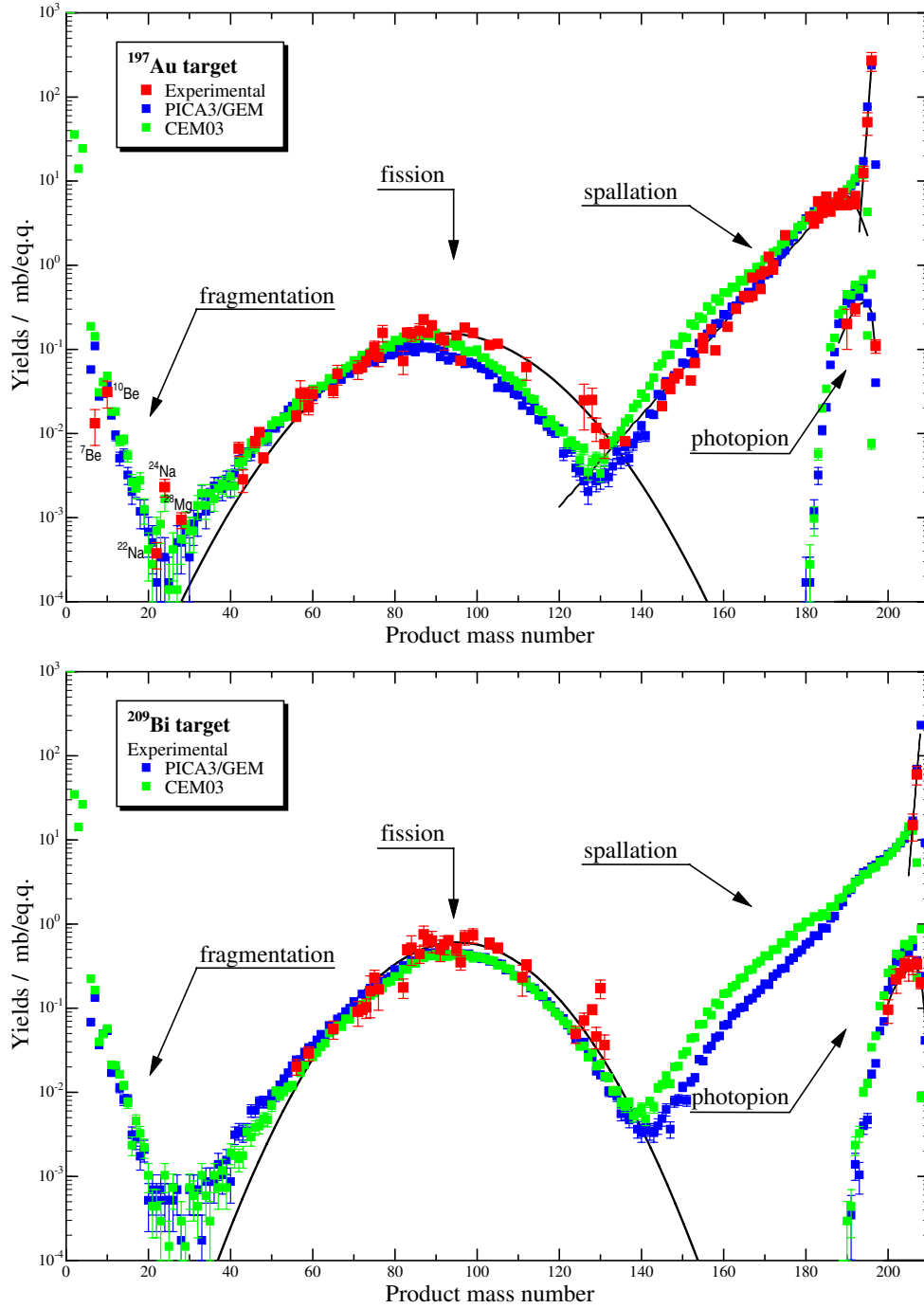


Figure 13: Comparison of CEM03 results for the isotopic yields of products produced by bremsstrahlung reactions on ^{197}Au and ^{209}Bi at $E_0 = 1$ GeV with experimental data [202, 203], [213]–[216] and calculations by PICA3/GEM [201]. The experimental yields from fission of ^{197}Au and ^{209}Bi are from Ref. [213]; those by spallation on ^{197}Au are from Refs. [214, 216]; those by fragmentation of ^{197}Au are from Ref. [215]; the PICA3/GEM results are from several publications of Prof. Sakamoto’s group and are presented in Fig. 18 of the review [195] with the corresponding citations. The mass yields for the fission products shown by black curves represent approximations based on experimental data obtained in Refs. [202, 203]. We thank Dr. Hiroshi Matsumura for making this figure for us by adding our CEM03 results to Fig. 18 of the review [195].

Our preliminary analysis shows that CEM03 also allows us to describe the recoil properties (forward and backward product yields, their F/B ratio, and mean kinetic energies) of nuclides produced in bremsstrahlung-induced reactions on medium and heavy targets at intermediate energies (see [196] and reference therein). We plan to publish our analysis in a future paper. Here we present only several predictions by CEM03 for the reaction of $E_0 = 1$ GeV bremsstrahlung photons on Au, as we find such results informative and useful to better understand the mechanisms of nuclear reactions.

Due to the momentum transferred by the bombarding gammas to the nuclear target, one may expect that most of the spallation products would fly in the forward direction in the laboratory system. The lower-right plot in Fig. 14 shows the mean laboratory angle Θ of all products as a function of A . We see that the mean angle of most spallation products is predicted by CEM03 to be between 72 and 80 degrees. (It is not equal to 0 degrees, as the probability of projectiles to have an impact parameter exactly equal to zero is equal to zero, and photons hit more often the periphery of the nucleus rather than its center.) The black solid curve in the upper-left plot of Fig. 14 shows the yield of all products as a function of A , the same results compared in Fig. 13 with experimental data and calculations by PICA3/GEM. Besides the total yield, this plot shows also its components from nuclides produced in the forward (long-dashed red line) and backward (blue dashed line) directions. One can see that for all the spallation isotopes, the cross sections for the forward products are about a factor of two higher than for backward products, in complete accordance with the available experimental data (see the review [196] and references therein). But the situation changes completely for fission products: The momenta of the fissioning nuclei is small, their mean kinetic energy in the laboratory system is a few MeV (see the upper-right plot in Fig. 14), that is much less than the kinetic energy from several tens to about a hundred MeV that fission fragments receive due to the Coulomb repulsion of the fragments. If we neglect the effects of angular momentum, the fission fragments would be distributed isotropically in the system of the fissioning nucleus, and the small momentum of the fissioning nuclei makes this distribution almost isotropic also in the laboratory system. The upper left plot of Fig. 14 shows that predicted yields for the fission fragments in the forward and backward directions are almost the same, *i.e.*, the F/B ratio for the fission fragments is almost equal to one, again in complete agreement with the available experimental data (see [196] and references therein).

The mean kinetic energy of the forward products shown in the upper-right plot of Fig. 14 is only very slightly higher than that of the backward products (the momenta of fissioning nuclei are low, as discussed above), with a little higher effect for the spallation products than for fission fragments, as is to be expected. Due to this fact and to the near isotropy of the fission fragments, some fission fragments may have their mean velocity in the direction opposite the beam, as can be seen from in the lower-left plot of this figure.

It is much more informative to study the F/B problem considering the forward and backward cross sections for every product separately, as shown in Figs. 15 and 16, rather than addressing only the A-distribution of their yields. Whereas the Z-averaged A-dependence of the F/B ratio is about a factor of two for all the spallation region (see also Fig. 17), the situation changes for individual isotopes. The cross sections of forward-emitted isotopes are still about a factor of two higher than the backward cross sections for most of the spallation products, but their ratio is much higher for Ho and Rh, and depends strongly on the mass numbers of the products. Ho and Rh are “photopion” products produced via $(\gamma, \pi^- xn)$ and $(\gamma, 2\pi^- xn)$, respectively, with emission of only a few neutrons in addition to the pions. When the number of emitted neutrons is small, the product “remembers” the momentum transferred to the target by the projectile, and such neutron-rich products go mainly forward, with a ratio F/B up to ten or higher. On the contrary, in reactions where many neutrons are emitted approximately isotropically, the residual nucleus has lost most of its “memory” of the initial momentum. Therefore the neutron-deficient products from such reactions have a smaller F/B ratio,

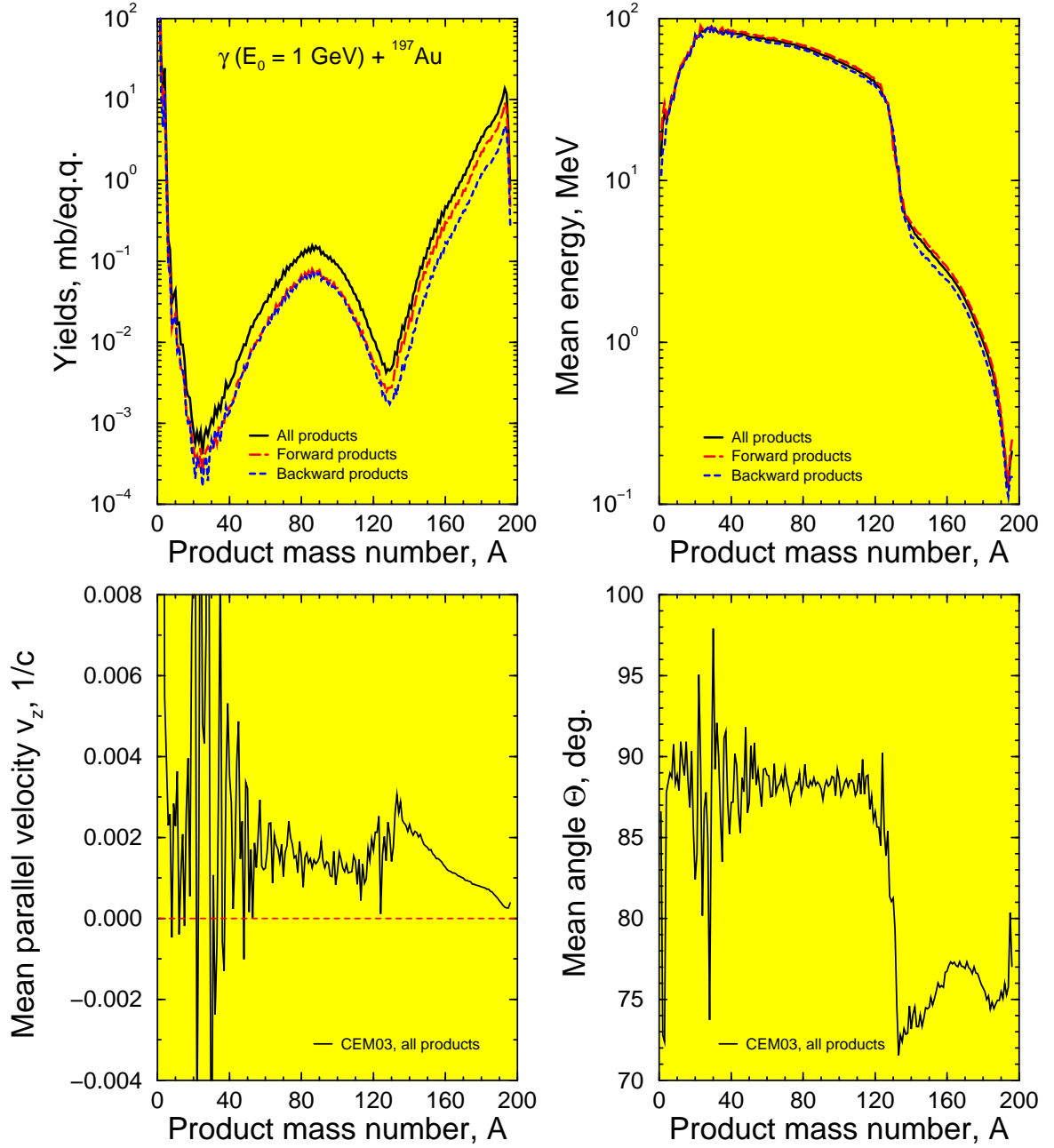


Figure 14: Results by CEM03 for 1 GeV bremsstrahlung-induced reactions on Au. **Upper left plot:** mass yield of all products (black line), isotopes produced in the forward laboratory direction (long-dashed red line), and backward products (dashed blue line); **Upper right plot:** mean laboratory kinetic energy of all products (black line) and of only forward (long-dashed red line) and backward products (dashed blue line); **Lower left plot:** mean laboratory velocity v_z of all products in the beam direction; **Lower right plot:** mean laboratory angle Θ of all products as a function of A . The big fluctuations in the values of v_z and Θ for masses around $A = 20$ and 130 do not provide real physical information, as they are related to the limited statistics of our Monte Carlo simulation caused by the very low yield of isotopes at the border between spallation and fission, and at that between fission and fragmentation. Our calculation provides only a few (or even one) isotopes of a given A in these mass regions, and mean values for such events do not have any significance.

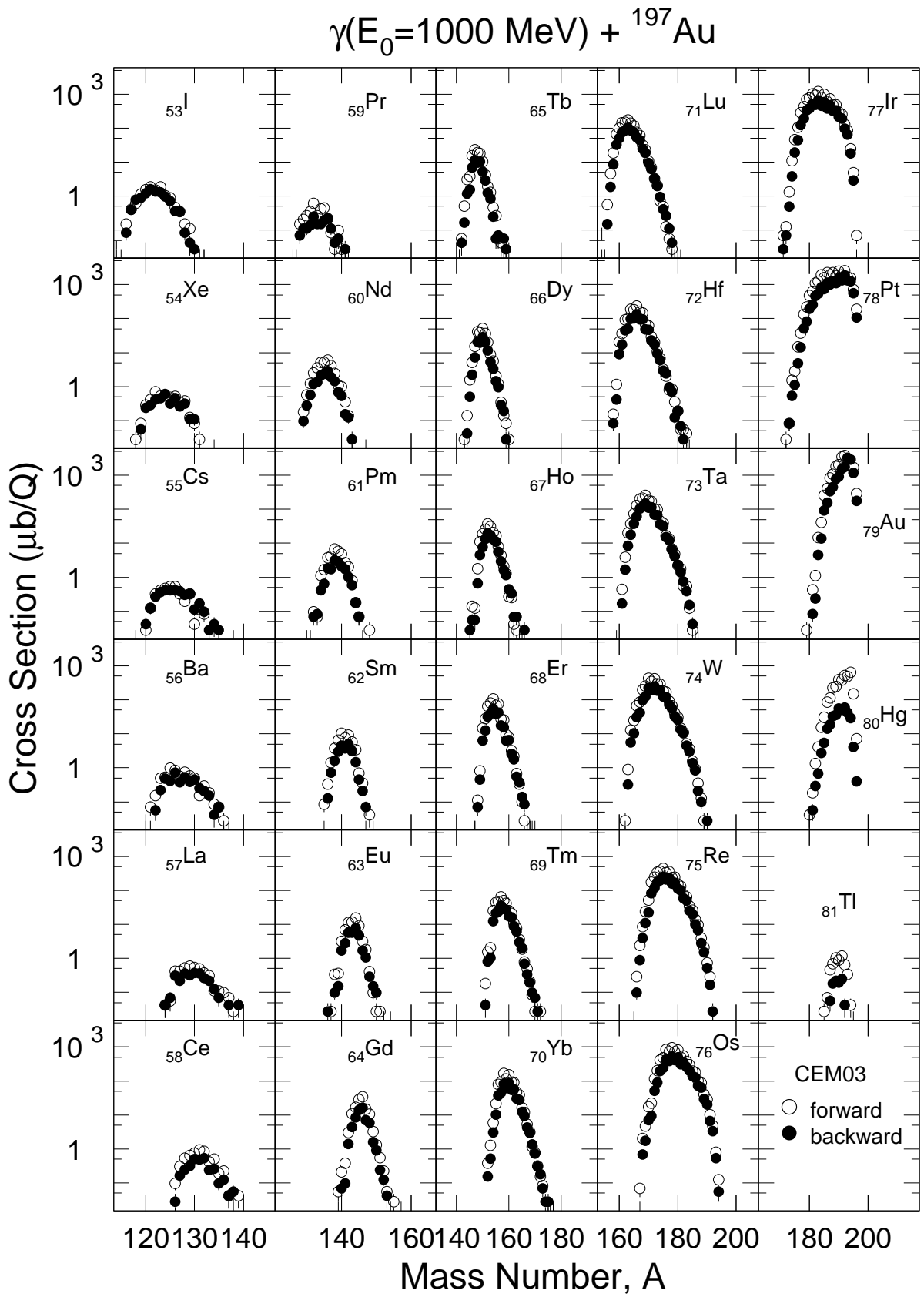


Figure 15: Predicted cross sections of the spallation products from the $E_0 = 1 \text{ GeV}$ bremsstrahlung photon-induced reaction on Au: Open circles show the yield of the products produced in the forward direction in the laboratory system, while the black circles show results for backward products.

$\gamma(E_0=1000 \text{ MeV}) + {}^{197}\text{Au}$, CEM03

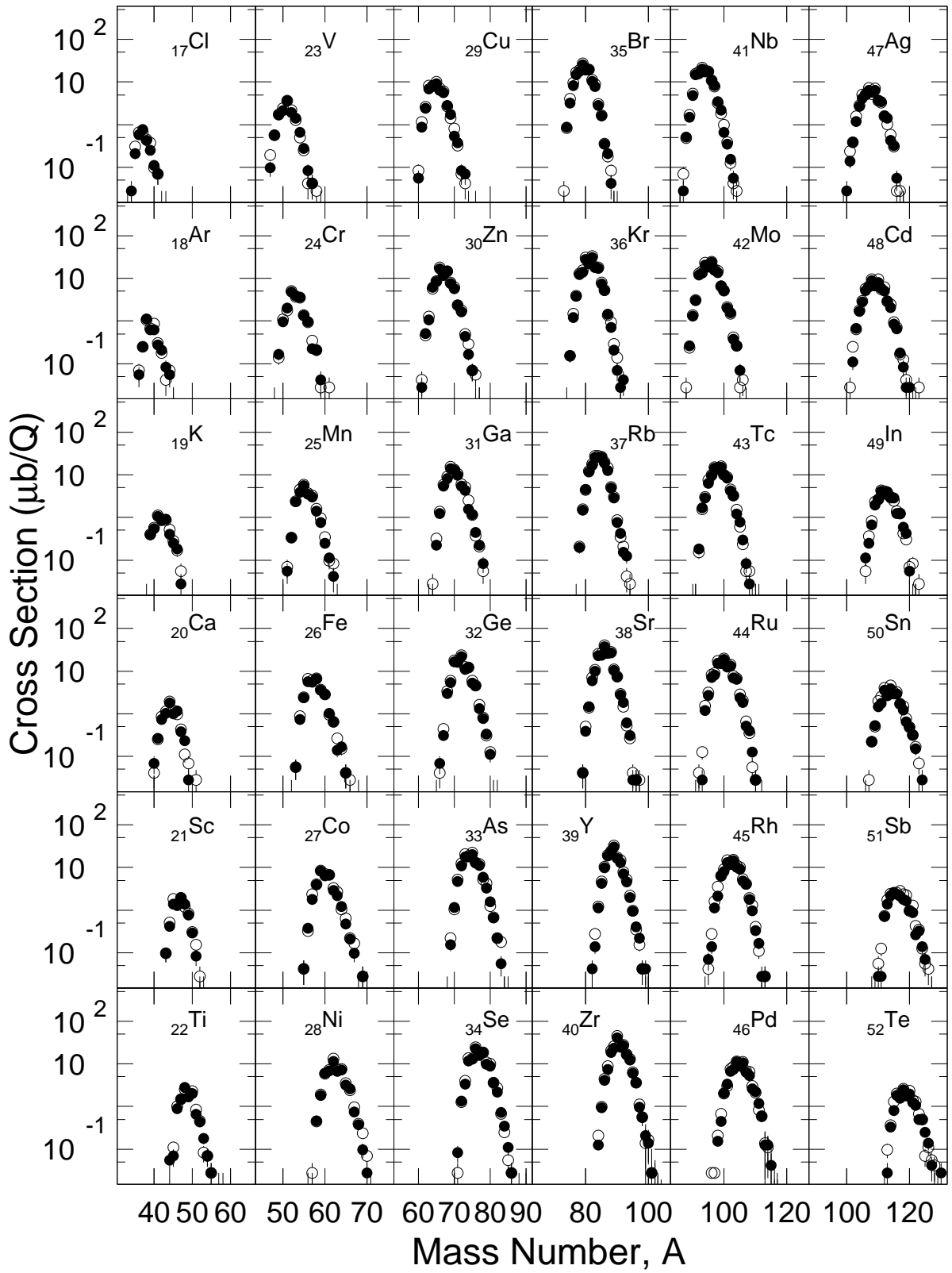


Figure 16: The same as Fig. 15, but for fission and fragmentation products.

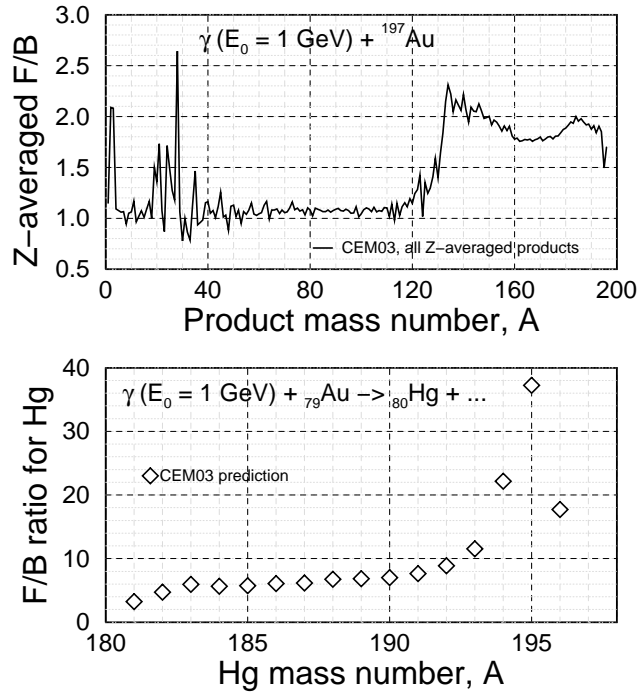


Figure 17: **Upper plot:** Z-averaged A-dependence of the F/B ratio of the forward product cross sections to the backward ones, as predicted by CEM03 for the reaction of $E_0 = 1$ GeV bremsstrahlung photons on Au. **Lower plot:** The F/B ratio of the Hg isotopes produced in the same reaction as a function of the mass number of the Hg nuclei.

usually around a factor of two. The farther away from the target are the products, the smaller is this effect; for products with $Z \lesssim 70$, it practically disappears. Approaching the border of the transition between spallation and fission products, the F/B ratio decreases and for Ce, La, Ba, Cs, Xe, and I nuclei shown in the left column of Fig. 15, the F/B ratio becomes almost equal to one and remains so for all the fission products shown in Fig. 16.

The Z-averaged F/B ratio for all nuclides of a given A as a function of A is presented in the upper plot of Fig. 17. The lower plot of this figure shows the F/B ratio for isotopes of Hg: One can see that it decreases from about thirty-seven for neutron-rich ${}^{195}\text{Hg}$ to about three for neutron-deficient ${}^{181}\text{Hg}$.

We think that analysis of such recoil characteristics is quite informative not only for photonuclear reactions, but also for proton-induced and other types of reactions. Analysis of experimental data for such characteristics would allow us to understand better the mechanisms of nuclear reactions and may help us to distinguish the fission processes from the fragmentation (or evaporation) ones in production of heavy fragments from reactions on medium-mass targets, like Fe (see discussion of this problem in [1, 2]). New measurements on the recoil properties from reactions with any type of projectiles, including bremsstrahlung photons, would be very useful.

Conclusions

The 2003 versions of the codes CEM2k+GEM2 and LAQGSM, CEM03 and LAQGSM03, are extended to describe photonuclear reactions. Both our models consider photoproduction of at most two pions, which limits their reliable application to photon energies up to only about 1.5 GeV. The present version of our models do not consider photoabsorption in the GDR region, which defines the lower limit of the photon energy to about 30 MeV. Nevertheless, developing and incorporating into CEM03 a routine based on the phenomenological systematics for the total photoabsorption cross section by Kossov allow us to enlarge the region of applicability of CEM03 and to get quite reasonable results for applications both in the GDR region and above 1.5 GeV.

As shown by several examples, CEM03 and LAQGSM03 allow us to describe reasonably well, and better than with their precursors, many photonuclear reactions needed for applications, as well as to analyze mechanisms of photonuclear reactions for fundamental studies. But our models still have several problems. Fig. 18 shows examples of such problems on proton and deuteron spectra from reactions induced by 60 MeV monoenergetic photons on Ca: One can see that both CEM03 and LAQGSM03 describe reasonably well the shape of the proton spectrum, but their absolute values differ by more than a factor of two. This is because the CEM03 results are normalized to the total photoabsorption cross section predicted by the Kossov systematics, which gives 3.49 mb for this reaction, while the LAQGSM03 results are normalized to the Monte-Carlo-calculated total photoabsorption cross section of 8.5 mb. If we refer to Fig. 4, we see that the Kossov systematics for the reaction $\gamma + \text{Ca}$ predict values that are a factor of two below available experimental data at energies around 60 MeV. This explains the difference we get between the CEM03 and LAQGSM03 results shown in Fig. 18, and suggest that the Kossov systematics should be further improved. Even allowing for this normalization problem, both codes appear to underestimate the cross sections for the higher-energy protons.

A further problem shown in Fig. 18 is for the spectra of deuterons. The predicted spectra of deuterons differ both in their shapes and absolute values for the two codes. CEM03 and LAQGSM03 have different intranuclear-cascade models, leading after the INC stage of any reaction to different average values for A , Z , and E of the excited nuclei, as a starting point for the preequilibrium and evaporation stages of reactions, where most of the deuterons are produced. This explains the difference in the deuteron spectra predicted by the two codes and suggests that further work to improve the description of complex-particle emission is necessary.

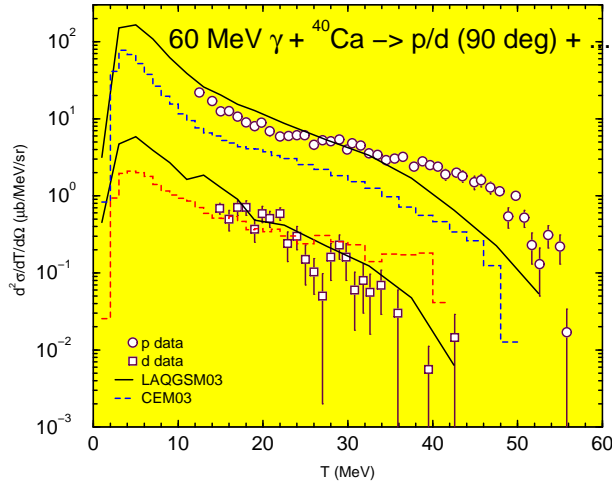


Figure 18: Examples of two problems with the current versions of our codes: proton and deuteron spectra at 90° from the reaction 60 MeV $\gamma + \text{Ca}$. Symbols are experimental data from [218], solid lines and dashed histograms are results from LAQGSM03 and CEM03, respectively. The CEM03 spectra are normalized to the total absorption cross section as predicted by Kossov's systematics, equal to 3.49 mb for this reaction, while the LAQGSM03 spectra are normalized to the Monte-Carlo total absorption cross section calculated by that code to be equal to 8.5 mb.

The overestimation of the high-energy tail of the deuteron spectrum by CEM03 is partially related with an imperfect description of the preequilibrium emission of d from this reaction, due to an excessively simplified estimation of the probability of several excited nucleons (exitons) coalescing into a complex particle that can be emitted during the decay of the excited nuclei produced after the cascade.

We plan to address these problem in the future. In addition, we plan to extend our models to describe photoabsorption in the GDR region, as discussed previously, and to extend our models to describe photonuclear reactions at energies of 10 GeV or more.

Our present study suggests that analyzing characteristics of recoil nuclei produced by photonuclear and other types of reactions is a powerfool tool to understand mechanisms of nuclear reactions. We encourage future measurements of such characteristics both for photonuclear and proton- or/and

nucleus-induced reactions.

Acknowledgements

We thank Dr. Kumataro Ukai for providing us with numerical values of single pion photoproduction cross sections from their compilation [36]. We are grateful to Dr. Igor Pshenichnov for sending us the γp and γn event generators used in their Moscow photonuclear reaction INC [33]. We thank Prof. Koh Sakamoto and Drs. Hiroshi Matsumura, Hiromitsu Haba, and Yasuji Oura for providing us with their publications and numerical tables of their measured data, as well as for useful discussions, help in drawing several figures for us, and their interest in our modeling.

This work was partially supported by the US Department of Energy, the Moldovan-US Bilateral Grants Program, CRDF Project MP2-3045-CH-02, and the NASA ATP01 Grant NRA-01-01-ATP-066.

References

- [1] S. G. Mashnik, K. K. Gudima, A. J. Sierk, and R. E. Prael, “Improved Intranuclear Cascade Models for the Codes CEM2k and LAQGSM,” LANL Research Note X-5-RN (U) 04-08, February 10, 2004; LA-UR-04-0039, Los Alamos (2004); *Proc. Int. Conf. on Nuclear Data for Sci. & Techn. (ND2004)*, September 26–October 1, 2004, Santa Fe, USA, 2004, in press; LA-UR-05-0711, Los Alamos (2005), E-print: nucl-th/0502019.
- [2] S. G. Mashnik, K. K. Gudima, R. E. Prael, A. J. Sierk, “Recent Developments in LAQGSM,” LA-UR-03-7277, Los Alamos (2003); talk presented at the *ICRS-10/RPS2004 Int. Conf.*, Funchal, Madeira, Portugal, May 9–14, 2004.
- [3] S. G. Mashnik, K. K. Gudima, R. E. Prael, and A. J. Sierk, “Analysis of the GSI A+p and A+A Spallation, Fission, and Fragmentation Measurements with the LANL CEM2k and LAQGSM Codes,” *Proc. Workshop on Nuclear Data for the Transmutation of Nuclear Waste*, GSI-Darmstadt, Germany, 2003, ISBN 3-00-012276-1, Eds: A. Kelic and K.-H. Schmidt, <http://www-wnt.gsi.de/tramu/>; E-print: nucl-th/0404018.
- [4] S. G. Mashnik and A. J. Sierk, “CEM2k—Recent Developments in CEM,” *Proc. AccApp2000 (Washington DC, USA, 2000)*, La Grange Park, IL, USA, 2001, pp. 328–341; E-print: nucl-th/0011064.
- [5] K. K. Gudima, S. G. Mashnik, and V. D. Toneev, “Cascade-Exciton Model of Nuclear Reactions,” *Nucl. Phys.* **A401**, 329–361 (1983).
- [6] S. G. Mashnik, K. K. Gudima, and A. J. Sierk, “Merging the CEM2k and LAQGSM Codes with GEM2 to Describe Fission and Light-Fragment Production,” *Proc. SATIF-6 (SLAC, USA, 2002)*, NEA/OECD, Paris, France, 2004, pp. 337–366; E-print: nucl-th/0304012.
- [7] S. G. Mashnik, A. J. Sierk, and K. K. Gudima, “Complex-Particle and Light-Fragment Emission in the Cascade-Exciton Model of Nuclear Reactions,” *Invited Talk at RPSD 2002 (Santa Fe, USA, 2002)*, LANL Report LA-UR-02-5185; E-print: nucl-th/0208048.
- [8] M. Baznat, K. Gudima, and S. Mashnik, “Proton-Induced Fission Cross Section Calculation with the LANL Codes CEM2k+GEM2 and LAQGSM+GEM2,” LANL Report LA-UR-03-3750, *Proc. AccApp’03 (San Diego, CA, 2003)*, La Grange Park, IL 60526, USA, 2004, pp. 976–985; E-print: nucl-th/0307014.
- [9] S. Furihata, “Statistical Analysis of Light Fragment Production from Medium Energy Proton-Induced Reactions,” *Nucl. Instr. Meth.* **B171**, 252–258 (2000); “The Gem Code Version 2 Users

- Manual,” Mitsubishi Research Institute, Inc., Tokyo, Japan (2001); Development of a Generalized Evaporation Model and Study of Residual Nuclei Production,” Ph.D. thesis, Tohoku University (2003).
- [10] K. K. Gudima, S. G. Mashnik, and A. J. Sierk, “User Manual for the Code LAQGSM,” LANL Report LA-UR-01-6804, Los Alamos (2001).
 - [11] N. V. Mokhov, K. K. Gudima, C. C. James, M. A. Kostin, S. G. Mashnik, E. Ng, J.-F. Ostiguy, I. L. Rakhno, A. J. Sierk, S. I. Striganov, “Recent Enhancements to the MARS15 Code,” FERMILAB-Conf-04/053-AD April 2004, LANL Report LA-UR-04-3047, E-print: nucl-th/0404084; *Proc. ICRS-10/RPS2004 Int. Conf.*, Funchal, Madeira, Portugal, May 9–14, 2004, in press.
 - [12] R. E. Prael, “Release Notes for LAHET Code System with LAHETTM Version 3.16,” X-Division Research Note X-5:RM (U) 01-29, LA-UR-01-1655, LANL, Los Alamos (2001).
 - [13] J. S. Hendricks, G. W. McKinney, L. S. Waters, T. L. Roberts, H. W. Egdorf, J. P. Finch, H. R. Trellue, E. J. Pitcher, D. R. Mayo, M. T. Swinhoe, S. J. Tobin, J. W. Durkee, F. X. Gallmeier, J.-C. David, W. B. Hamilton, and J. Lebenhaft, “MCNPX Extensions Version 2.5.0,” LANL Report LA-UR-04-0570 and references therein; <http://mcnp.x.lanl.gov/>.
 - [14] F. B. Brown, “Monte Carlo Methods & MCNP Code Development,” LANL Report LA-UR-04-2648, *Proc. PHYSOR-2004*, 4-29-2004; R. Arthur Forster, Lawrence J. Cox, Richard F. Barrett, Thomas E. Booth, Judith F. Breismeister, Forrest B. Brown, Jeffrey S. Buul, Gregg C. Geisler, John T. Goorley, Russell D. Mesteller, Susan E. Post, Richard E. Prael, Elizabeth C. Selcow, and Avneet Sood, “MCNPTM Version 5,” *NIM*, **B213**, 82-86 (2004); J. F. Briesmeister, Ed., “MCNP—A General Monte Carlo N-Particle Transport Code - Version 4C,” LANL Report LA-13709-M (March, 2000); www-xdiv.lanl.gov/x5/MCNP/.
 - [15] K. K. Gudima, A. S. Iljinov, and V. D. Toneev, “A Cascade Model for Photonuclear Reactions,” Communication JINR P2-4661, Dubna (1969).
 - [16] V. S. Barashenkov and V. D. Toneev, *Interaction of High Energy Particles and Nuclei with Atomic Nuclei*, (in Russian) Atomizdat, Moscow (1972).
 - [17] V. S. Barashenkov, F. G. Geregi, A. S. Iljinov, G. G. Jonsson, and V. D. Toneev, “A Cascade-Evaporation Model for Photonuclear Reactions,” *Nucl. Phys.* **A231**, 462–476 (1974).
 - [18] M. V. Kossov, “Approximation of Photonuclear Interaction Cross-Sections,” *Eur. Phys. J.* **A14**, 377–392 (2002).
 - [19] J. S. Levinger, “The High Energy Nuclear Photoeffect,” *Phys. Rev.* **84**, 43–51 (1951); *Nuclear Photo-Disintegration*, Oxford University Press (1960); see also “Modified Quasi-Deuteron Model,” *Phys. Lett.* **B82**, 181–182 (1979).
 - [20] W. O. Lock and D. F. Measday, *Intermediate Energy Nuclear Physics*, London, Methuen; [Distributed in the U.S.A. by Barnes and Noble, 1970].
 - [21] V. S. Barashenkov, K. K. Gudima, and V. D. Toneev, “Intranuclear Cascade Calculation Scheme,” [in Russian] JINR Communication P2-4065, Dubna, 1968.
 - [22] V. S. Barashenkov, K. K. Gudima, and V. D. Toneev, “Statistical Calculation of Inelastic Collisions of Fast Particles with Intranuclear Nucleons,” JINR Communication P2-4066, Dubna, 1968; *Acta Physica Polonica* **36**, 415–432 (1969) [in Russian].
 - [23] S. Eidelman *et al.* (Particle Data Group), “Review of Particle Physics,” *Phys. Lett.* **B592**, 1–1109 (2004); <http://pdg.lbl.gov>.
 - [24] S. J. Lindenbaum and R. M. Sternheimer, “Isobaric Nucleon Model for Pion Production in Nucleon-Nucleon Collisions,” *Phys. Rev.* **105**, 1874–1899 (1957).

- [25] V. S. Barashenkov, Le Van Ngok, L. G. Levchuk, Zh. Zh. Musul'manbekov, A. N. Sosnin, V. D. Toneev and S. Yu. Shmakov, "Cascade Program Complex for Monte-Carlo Simulation of Nuclear Processes Initiated by High Energy Particles and Nuclei in Gaseous and Condensed Matter," *JINR Communication R2-85-173*, Dubna (1985); V. S. Barashenkov, "Monte Carlo Simulation of Ionization and Nuclear Processes Initiated by Hadrons and Ion Beams in Media," *Comp. Phys. Communic.* **126**, 28–31 (2000).
- [26] Nikolai Amelin, "Physics and Algorithms of the Hadronic Monte-Carlo Event Generators1. Notes for a Developer," Preprint CERN/IT/99/6, CERN, Geneva (1999); <http://atlas.web.cern.ch/Atlas/GROUPS/SOFTWARE/OO/domains/simulation/G4PhysicsStudies/documentation/ameline/makebookphysics.html#tex2html1>.
- [27] S. G. Mashnik, *User Manual for the Code CEM95*, JINR, Dubna, USSR; OECD NEA Data Bank, Paris, France; <http://www.nea.fr/abs/html/iaea1247.html>; RSIC-PSR-357, Oak Ridge, USA (1995).
- [28] S. G. Mashnik and A.J. Sierk, "Improved Cascade-Exciton Model of Nuclear Reactions," *Proc. SARE-4*, Knoxville, TN, 1998, ORNL, 1999, pp. 29–51; E-print: nucl-th/9812069.
- [29] N. V. Mokhov, S. I. Striganov, A. Van Ginneken, S. G. Mashnik, A. J. Sierk, and J. Ranft, "MARS Code Development," *Proc. SARE-4*, Knoxville, TN, 1998; ORNL, 1999, pp. 87–99; E-print: nucl-th/9812038.
- [30] F. X. Gallmeier and S. G. Mashnik, "Photonuclear Physics Modules for MCNPX Above the Tabular Range," *Proc. AccApp00*, 2000, Washington, DC (USA), ANS, La Grange Park, IL, 2001, pp. 342–349.
- [31] Franz Gallmeier, "A Photoabsorption Cross Section Model for the Physics Models Regime in MCNPX," *Proc. ICRS-10/RPS 2004*, 2004, Funchal, Madeira, Portugal, <http://www.itn.mc.es.pt/ICRS-RPS/presentations.html>, in press.
- [32] A. S. Iljinov, M. V. Kazarnovsky, and E. Ya. Paryev, *Intermediate-Energy Nuclear Physics*, CRC Press, Boca Raton, 1994.
- [33] A. S. Iljinov, I. A. Pshenichnov, N. Bianchi, E. De Sanctis, V. Muccifora, M. Mirazita, and P. Rossi, "Extension of the Intranuclear Cascade Model for Photonuclear Reactions at Energies up to 10 GeV," *Nucl. Phys.* **A616**, 575–605 (1997).
- [34] T. Gabriel, G. Maino, and S. G. Mashnik, "Analysis of Intermediate Energy Photonuclear Reactions," JINR Preprint E2-94-424, Dubna, 1994; *Proc. XII Int. Sem. on High Energy Phys. Problems* Dubna, Russia, 1994, Eds. A. M. Baldin and V. V. Burov, Dubna, JINR Pub. Dep., JINR E1,2-97-79, pp. 309–318 (1997).
- [35] F. G. Gereghi, V. A. Zolotarevsky, K. K. Gudima, S. G. Mashnik, and L. V. Bordianu, "Calculation of Cross Sections for Photoneutron Reactions," Kishinev State University Report 01870081266, 1990, 125 p. [in Russian].
- [36] K. Ukai and T. Nakamura, "Data Compilation of Single Pion Photoproduction Below 2 GeV", INS-T-550, March 1997, Inst. for Nucl. Study, University of Tokyo, and private communication from K. Ukai to SGM (1997).
- [37] S. I. Alekhin, A. Baldini, P. Capiluppi, M. Cobal, V. V. Ezhela, V. Flaminio, G. Giacomelli, S. B. Lugovsky, G. Mandrioli, W. G. Moorhead, D. R. O. Morrison, N. Rivoire, A. M. Rossi, P. Serra, A. N. Tolstenkov, and O. P. Yushchenko, *Compilation of Cross-Sections IV: γ , μ , Λ , Σ , Ξ , and K_L^0 Induced Reactions*, CERN-HERA 87-01, 121 pp., CERN, Geneva, (2 February 1987); <http://www-lib.kek.jp/cgi-bin/kiss-prepri.v3?KN=199101079>.

- [38] D. W. Menze, W. Pfeil, and R. Wilcke, *Compilation of Pion Photoproduction Data*, Physics Data 7-1, Physikalisches Institut der Universität Bonn, Germany (1977), 306 pp.; “Compilation of Pion Photoproduction Data,” Eds., W. Pfeil, R. Wilcke, and D. W. Menze, Eggenstein-Leopoldshafen Karlsruhe Fachinformationszent. Kernforsch. Zentralstelle At. Energ. 1977, 315 pp.
- [39] H. Genzel, P. Joos, and W. Pfeil, *Photoproduction of Elementary Particles*, Landolt-Börnstein, Numerical Data and Functional Relationship in Science and Technology, New Series, Ed. in Chief, K.-H. Hellwege, Group I: Nuclear and Particle Physics, Vol. 8, Ed., H. Schöper, Springer-Verlag, Heidelberg, 1973, 341 pp.
- [40] E. Mazzucato, P. Argan, G. Audit, A. Bloch, N. de Botton, N. d’Hose, J. -L. Faure, M. L. Ghedira, C. Guerra, J. Martin, C. Schuhl, G. Tamas, and E. Vincent, “Precise Measurement of Neutral-Pion Photoproduction on the Proton near Threshold,” *Phys. Rev. Lett.* **57**, 3144–3147 (1986).
- [41] C. Ward, B. Kenton, and C. York, Photoproduction of π^0 from Hydrogen near the Second and Third Pion-Nucleon Resonances,” *Phys. Rev.* **159**, 1176–1186 (1967).
- [42] H. R. Crouch, Jr., R. Hargraves, B. Kendall *et al.* (*Cambridge Bubble Chamber Group*), “Analysis of $\gamma - p$ Reactions in a Hydrogen Bubble Chamber to 6.0 BeV: Cross Sections and Laboratory Distributions,” *Phys. Rev.* **155**, 1477–1488 (1967).
- [43] W. J. Podilsky, Thesis, University of California, Berkeley, 1971.
- [44] O. Bartholomy, V. Crede, H. van Pee, for the CB-ELSA Collaboration, “Neutral Pion Photoproduction off Protons in the Energy Range $0.3 \text{ GeV} < E_\gamma < 3 \text{ GeV}$,” E-print: hep-ex/0407022; <http://www-spires.dur.ac.uk/cgi-bin/hepdata/react3>.
- [45] M. Fuchs, J. Ahrens, G. Anton, R. Auerbeck, R. Beck, A. M. Bernstein, A. R. Gabler, F. Härter, *et al.*; “Neutral Pion Photoproduction from the Proton Near Threshold,” *Phys. Lett.* **B368**, 20–25 (1996); <http://www-spires.dur.ac.uk/cgi-bin/hepdata/tabkum/TABLE/9148/999/1/1>.
- [46] S. D. Ecklund and R. L. Walker, “ π^+ Photoproduction from Hydrogen at Laboratory Energies from 589 to 1269 MeV,” *Phys. Rev.* **159**, 1195–1209 (1967).
- [47] C. Betourne, J. C. Bizot, J. Perez-Y-Jorba, and D. Treille, “Photoproduction of Positive Pions from Hydrogen between 300 and 750 MeV,” *Phys. Lett.* **B24**, 590–593 (1967).
- [48] D. A. McPherson, D. C. Gates, R. W. Kenney, and W. P. Swanson, “Positive Photopion Production from Hydrogen Near Threshold,” *Phys. Rev.* **136**, B1465–B1471 (1964).
- [49] G. Fischer, G. von Holtey, G. Knop, and J. Stümpfig, “Angular Distributions of Pions from $\gamma + p \rightarrow \pi^+ + n$ at Photon Energies between 220 and 425 MeV,” *Z. Physik* **253**, 38–52 (1972).
- [50] T. Fujii, T. Kondo, F. Takasaki, S. Yamada, S. Homma, K. Huke, S. Kato, H. Okuno, I. Endo, and H. Fuji, “Photoproduction of Charged π Mesons from Protons and Neutrons in the Energy Range between 250 and 790 MeV,” *Nucl. Phys.* **B120**, 395–422 (1977).
- [51] M. MacCormick, G. Audit, N. d’Hose, L. Ghedira, V. Isbert, S. Kerhoas, L. Y. Murphy, G. Tamas, P. A. Wallace, S. Altieri, A. Braghieri, P. Pedroni, T. Pinelli, J. Ahrens, R. Beck, J. R. M. Annand, R. A. Crawford, J. D. Kellie, I. J. D. MacGregor, B. Dolbilkin, and A. Zabrodin, “Total Photoabsorption Cross Sections for ^1H , ^2H , and ^3He from 200 to 800 MeV,” *Phys. Rev. C* **53**, 41–49 (1996); EXFOR File M0519.
- [52] “Data Files and Plots of Cross Sections and Related Quantities. Hadron(Photon)-Hadron(Photon) Collisions,” Courtesy of the COMPAS Group, IHEP, Protvino, Russia, <http://wwwppds.ihep.su:8001/hadron.html>; <http://pdg.lbl.gov/2002/contents-plots.html>.

- [53] R. Bernabei, A. Incicchitti, M. Mattioli, P. Picozza, D. Prosperi, L. Casano, S. d'Angelo, M. P. De Pascale, C. Schaerf, G. Giordano, G. Matone, S. Frullani, and B. Girolami, "Total Cross Section for Deuteron Photodisintegration between 15 and 75 MeV," *Phys. Rev. Lett.* **57**, 1542–1545 (1986).
- [54] J. Arends, H. J. Gassen, A. Hegerath, B. Mecking, G. Nöldeke, P. Prenzel, T. Reichelt, A. Voswinkel, and W. W. Sapp, "Experimental Investigation of Deuteron Photodisintegration in the Δ -Resonance Region," *Nucl. Phys.* **A412**, 509–522 (1984).
- [55] H. O. Meyer, J. R. Hall, M. Hugli, H. J. Karwowski, R. E. Pollock, and P. Schwandt, "Neutron-Proton Radiative Capture Cross Section at $T_n = 185$ MeV," *Phys. Rev. C* **31**, 309–317 (1985).
- [56] P. Levi Sandri, M. Anghinolfi, N. Bianchi, G. P. Capitani, P. Corvisiero, E. De Sanctis, C. Guaraldo, V. Lucherini, V. Muccifora, E. Polli, A. R. Reolon, G. Ricco, P. Rossi, M. Sanzone, and M. Taiuti, "Differential Cross Section at Forward and Backward Angles for Deuteron Photodisintegration at Intermediate Energies," *Phys. Rev. C* **39**, 1701–1708 (1989), and compilation of previous measurements therein.
- [57] J. M. Cameron, C. A. Davis, H. Fielding, P. Kitching, J. Pasos, J. Soukup, J. Uegaki, J. Wesick, H. S. Wilson, R. Abegg, D. A. Hutcheon, C. A. Miller, A. W. Stetz, and I. L. van Heerden, "Radiative Capture of Polarized Neutrons by Hydrogen below the Pion Production Threshold," *Nucl. Phys.* **A458**, 637–651 (1986).
- [58] M. Hugli, J. M. Cameron, M. Ahmad, J. Collot, G. Gaillard, J. S. Wesick, G. W. R. Edwards, H. Fielding, D. A. Hutcheon, R. Abegg, C. A. Miller, P. Kitching, N. E. Davison, N. R. Stevenson, and I. J. van Heerden, "Radiative Capture of Polarized Neutrons above Pion Production Threshold," *Nucl. Phys.* **A472**, 701–717, (1987).
- [59] P. Dougan, V. Ramsay, and W. Stiefler, "Cross-Sections for Deuteron Photo-Disintegration from 74 to 241 MeV," *Z. Physik* **280**, 341–348 (1977).
- [60] D. M. Skopik, Y. M. Shin, M. C. Phenneger, and J. J. Murphy, II, "Photodisintegration of Deuterium Determined from the Electrodissociation Process," *Phys. Rev. C* **9**, 531–536 (1974).
- [61] R. L. Anderson, and R. Prepost, and B. H. Wiik, "Photodisintegration of the Deuteron from 220 to 340 MeV," *Phys. Rev. Lett.* **22**, 651–654 (1969).
- [62] J. Buon, V. Gracco, J. Lefrancois, P. Lehmann, B. Merkel, Ph. Roy, "Photodisintegration of the Deuteron from 140 to 400 MeV," *Phys. Lett.* **B26**, 595–597 (1968).
- [63] J. Ahrens, H. B. Eppler, H. Gimm, M. Kröning, P. Riehn, H. Wäffler, A. Zieger, and B. Ziegler, "Photodisintegration of the Deuteron at 15–25 MeV Photon Energy," *Phys. Lett.* **B52**, 49–50 (1974).
- [64] E. A. Whalin, Barbara Dwight Schriever, and A. O. Hanson, "Photodisintegration of Deuterium by 60- to 250-MeV X-Rays," *Phys. Rev.* **101**, 377–384 (1956).
- [65] J. C. Keck and A. V. Tollestrup, "Photodissociation of the Deuteron from 150 to 450 MeV," *Phys. Rev.* **101**, 360–370 (1956).
- [66] J. Halpern and E. V. Weinstock, "Photodisintegration of the Deuteron at 20 MeV," *Phys. Rev.* **91**, 934–939 (1953), and compilation of previous measurements therein.
- [67] E. De Sanctis, M. Anghinolfi, G. P. Capitani, P. Corvisiero, P. Di Giacomo, C. Guaraldo, V. Lucherini, E. Polli, A. R. Reolon, G. Ricco, M. Sanzone, and A. Zucchiatti, "Differential Cross Section for the $2H(\gamma, p)n$ Reaction between 100 and 255 MeV," *Phys. Rev. C* **34**, 413–421 (1986), and compilation of previous measurements therein.
- [68] EXFOR Data Base, *e.g.* at: <http://www.nea.fr/html/dbdata/x4/x4ret.html>.

- [69] K. Y. Hara, H. Utsunomiya, S. Goko, H. Akimune, T. Yamagata, M. Ohta, H. Toyokawa, K. Kubo, A. Uritani, Y. Shibata, Y.-W. Lui, and H. Ohgaki, “Photodisintegration of Deuterium and Big Bang Nucleosynthesis,” *Phys. Rev. D* **68**, 072001 (2003).
- [70] R. Bernabei, A. Chisholm, S. d’Angelo, M. P. De Pascale, P. Picozza, C. Schaerf, P. Belli, L. Casano, A. Incicchitti, D. Prosperi, and B. Girolami, “Measurement of the ${}^4\text{He}(\gamma, p){}^3\text{H}$ Total Cross Section and Charge Symmetry,” *Phys. Rev. C* **38**, 1990–1995 (1988).
- [71] Y. Birenbaum, S. Kahane, and R. Moreh, “Absolute Cross Section for the Photodisintegration of Deuterium,” *Phys. Rev. C* **32**, 1825–1829 (1985).
- [72] R. Moreh, T. J. Kennett, and W. V. Prestwich, “ ${}^2\text{H}(\gamma, n)$ absolute cross section at 2754 keV,” *Phys. Rev. C* **39**, 1247–1250 (1989).
- [73] A. Braghieri, L. Y. Murphy, J. Ahrens, G. Audit, N. d’Hose, V. Isbert, S. Kerhoas, M. MacCormick, P. Pedroni, T. Pinelli, G. Tamas, and A. Zabrodin, “Total Cross Section Measurement for the Three Double Pion Photoproduction Channels on the Proton,” *Phys. Lett.* **B363**, 46–50 (1995); <http://www-spires.dur.ac.uk/cgi-bin/hepdata/tabkum/TABLE/8626/999/1/1>.
- [74] K. Abe, T. C. Bacon, J. Ballam *et al.* (*SLAC Hybrid Facility Photon Collaboration*), “Study of the $\rho'(1600)$ Mass Region Using $\gamma p \rightarrow \pi^+ \pi^- p$ at 20 GeV,” *Phys. Rev. Lett.* **53**, 751–754 (1984); <http://www-spires.dur.ac.uk/cgi-bin/hepdata/tabkum/TABLE/4925/999/1/1>.
- [75] A. Piazza, G. Susinno, L. Fiore, G. Gialanella, E. Lodi-Rizzini, G. C. Mantovani, A. Piazzoli, F. Carbonara, G. Palomba-Nicodemi, and R. Rinzivillo, “Total Cross-Sections of $\pi^+ \pi^-$ and $\pi^- \pi^0$ Photoproduction on Neutron in Deuterium Bubble Chamber up to 900 MeV,” *Lett. Nuovo Cimento* **3**, 403–408 (1970).
- [76] R. Erbe *et al.* (*ABBHHM Collaboration*), “Photoproduction of Meson and Baryon Resonances at Energies up to 5.8 GeV,” *Phys. Rev.* **175**, 1669–1696 (1968).
- [77] M. Kotulla, J. Ahrens, J. R. M. Annand, R. Beck, D. Hornidge, S. Janssen, B. Krusche, J. C. McGeorge, I. J. D. MacGregor, J. G. Messchendorp, V. Metag, R. Novotny, M. Pfeiffer, R. O. Owens, M. Rost, S. Schadmand, and D. P. Watts, “Double π^0 Photoproduction off the Proton at Threshold,” *Phys. Lett.* **B578**, 63–68 (2004); <http://www-spires.dur.ac.uk/cgi-bin/hepdata/tabkum/TABLE/10996/999/1/1>.
- [78] M. Wolf, J. Ahrens, R. Beck, V. Hejny, J. D. Kellie, M. Kotulla, B. Krusche, V. Kuhr, R. Leukel, V. Metag, J. C. Nacher, R. Novotny, V. Olmos de León, R. O. Owens, F. Rambo, A. Schmidt, M. Schumacher, U. Siodlaczek, H. Ströher, J. Weiß, and F. Wissmann, “Photoproduction of Neutral Pion Pairs from the Proton,” *Eur. Phys. J.* **A9**, 5–8 (2000).
- [79] F. Härter, J. Ahrens, R. Beck, B. Krusche, V. Metag, M. Schmitz, H. Ströher, Th. Walcher, and M. Wolf, “Two Neutral Pion Photoproduction off the Proton between Threshold and 800 MeV,” *Phys. Lett.* **B401**, 229–233 (1997).
- [80] J. Ahrens *et al.* (*GDH and A2 Collaboration*), “Helicity Dependence of the $\vec{\gamma} p \rightarrow n \pi^+ \pi^0$ Reaction in the Second Resonance Region,” *Phys. Lett.* **B551**, 49–55 (2003).
- [81] W. Langgärtner, J. Ahrens, R. Beck, V. Hejny, M. Kotulla, B. Krusche, V. Kuhr, R. Leukel, J. D. MacGregor, J. G. Messchendorp, V. Metag, R. Novotny, V. Olmos de León, R. O. Owens, F. Rambo, S. Schadmand, A. Schmidt, U. Siodlaczek, H. Ströher, J. Weiß, F. Wissmann, and M. Wolf, “Direct Observation of a ρ Decay of the $D_{13}(1520)$ Baryon Resonance,” *Phys. Rev. Lett.* **87**, 052001 (2001).
- [82] K.-H. Schmidt, personal Web page: <http://www-wnt.gsi.de/kschmidt/>.
- [83] R. W. Clifton, E. Gabathuler, L. S. Littenberg, R. Marshall, S. E. Rock, J. C. Thompson, D. L. Ward, and G. R. Brookes, “Search for $\Delta I = 2$ Electromagnetic Currents in Pion Photoproduction,” *Phys. Rev. Lett.* **33**, 1500–1503 (1974).

- [84] H. Genzel, E. Hilger, G. Knop, H. Kemen, and R. Wedemeyer, “Photoproduction of Neutral Pions on Hydrogen Below 500 MeV,” *Z. Phys.* **268**, 43–50 (1974).
- [85] G. Fischer, H. Fischer, G. von Holtey, H. Kämpgen, G. Knop, P. Schulz, H. Wessels, W. Braunschweig, H. Genzel, and R. Wedemeyer, “Photoproduction of Neutral Pions on Hydrogen at Photon Energies Between 200 and 440 MeV,” *Nucl. Phys.* **B16**, 93–101 (1970).
- [86] W. S. McDonald, V. Z. Peterson, and D. R. Corson, “Photoproduction of Neutral Pions from Hydrogen at Forward Angles from 240 to 480 MeV,” *Phys. Rev.* **107**, 577–585 (1957).
- [87] Yu. A. Alexandrov, V. A. Kozlov, and V. V. Pavlovskaya, “Study of the Photoproduction of Neutral Pions in Hydrogen in the Region of the $\Delta(1232)$ Resonance,” *Yad. Fiz.* **28**, 670–674 (1978) [*Sov. J. Nucl. Phys.* **28**, 344–346 (1978)].
- [88] R. L. Walker, D. C. Oakley, and A. V. Tollestrup, “Photoproduction of Neutral Pions in Hydrogen: $p - \gamma$ Coincidences,” *Phys. Rev.* **97**, 1279–1282 (1955).
- [89] Yoshioka 1977 INS-281 data (no detailed reference) tabulated at: <http://www-spires.dur.ac.uk/hepdata/reac2.html>.
- [90] H. Becks, P. Feller, D. Menze, U. Opara, W. Schultz, and W. J. Schwill, “Backward Photoproduction of Neutral Pions off Hydrogen at Photon Energies Between 0.4 and 2.2 GeV,” *Nucl. Phys.* **B60**, 267–276 (1973).
- [91] S. Almehed, G. von Dardel, G. Jarlskog, L. Jönsson, B. Lörstad, J. Palmer, R. Peterson, and L. Svensson, “Measurements on the Differential Cross Section of the π^0 -Production on Hydrogen,” *Physica Scripta* **13**, 321–326 (1976).
- [92] H. De Staebler, Jr., E. F. Erickson, A. C. Hearn, and C. Schaere, “Photoproduction of π^0 from Hydrogen near the Second Pion-Nucleon Resonance,” *Phys. Rev.* **140**, B336–B348 (1965).
- [93] P. Feller, H. Herr, E. Hilger, V. Kadansky, D. Menze, Th. Miczaika, U. Opra, and W. J. Schwill, “Photoproduction of Neutral Pions off Hydrogen at Photoenergies Between 0.55 and 2.2 GeV at a CM-Angle of 120° ,” *Phys. Lett.* **B49**, 197–200 (1974).
- [94] Wolverson 1968 data (no detailed reference) tabulated at: <http://www-spires.dur.ac.uk/hepdata/reac2.html>.
- [95] Wermes 1978, Bonn-IR-78-9 data (no detailed reference) tabulated at: <http://www-spires.dur.ac.uk/hepdata/reac2.html>.
- [96] B. Delcourt, J. Lefrançois, G. Parrou, J. P. Perez-Y-Jorba, and G. Sauvage, “ π^0 Photoproduction on Proton at Backward Angles Between 700 MeV and 1150 MeV,” *Phys. Lett.* **B29**, 70–74 (1960).
- [97] R. M. Worlock, “Photoproduction of Neutral Pions at Energies 600 to 800 MeV,” *Phys. Rev.* **117**, 537–543 (1960).
- [98] D. Husmann, W. Jansen, B. Löhr, and H. Schilling, “Forward Photoproduction of Neutral Pions on Protons in the Third Resonance Region,” *Nucl. Phys.* **B126**, 436–442 (1977).
- [99] J. S. Barton, P. S. L. Booth, L. J. Carroll, J. R. Holt, J. N. Jackson, G. Moscatti, and J. R. Wormald, “The Photoproduction of Neutral Pions from Protons Between 0.7 GeV and 1.7 GeV,” *Nucl. Phys.* **B84**, 449–466 (1975).
- [100] H. E. Jackson, J. W. DeWire, and R. M. Littauer, “Photoproduction of π^0 Mesons from Hydrogen in the Region 900 to 1200 MeV,” *Phys. Rev.* **119**, 1381–1384 (1960).
- [101] K. H. Althoff, M. Gies, O. Kaul, K. Königsmann, D. Menze, W. Meyer, T. Miczaika, E. Roderburg, and W. Schwill, “Photoproduction of Neutral Pions in the Region of the Four Nucleon Resonance,” *Z. Phys.* **C1**, 257–258 (1979).

- [102] Lohr 1970, Bonn-1-98 data (no detailed reference) tabulated at: <http://www-spires.dur.ac.uk/hepdata/reac2.html>.
- [103] M. I. Adamovich, V. G. Larionova, R. A. Latypova, A. I. Lebedev, S. P. Kharlamov, and F. R. Yagudina, “Investigation of the Angular Dependence of the Cross Section for Photoproduction of Charged Pions on Nucleons,” *Zh. Exp. Teor. Fiz.* **53**, 528–538 (1967).
- [104] M. I. Adamovich, E. G. Gorzhetskaya, V. G. Larionova, V. M. Popova, S. P. Kharlamov, and F. R. Yagudina, “Photoproduction of Charged π -Mesons Near the Threshold,” *Zh. Exp. Teor. Fiz.* **11**, 1078–1083 (1960).
- [105] K. Althoff, “Photoproduction of Positive Pions Between 200 and 260 MeV at Fixed Momentum Transfer,” *Z. Phys.* **175**, 34–36 (1963).
- [106] D. Freytag, W. J. Schulle, and R. J. Wedemeyer, “Measurements of Cross-Sections for the Photoproduction of Positive Pions on Hydrogen in the Region of the First Resonance,” *Z. Phys.* **186**, 1–22 (1965).
- [107] M. Beneventano, G. Bernardini, D. Carlson-Lee, G. Stoppini, and L. Tau, “Differential Cross-Sections for Photoproduction of Positive Pions in Hydrogen,” *Nuovo Cimento* **4**, 323–356 (1956).
- [108] R. L. Walker, J. G. Teasdale, V. Z. Peterson, and J. I. Vette, “Photoproduction of Positive Pions in Hydrogen-Magnetic Spectrometer Method,” *Phys. Rev.* **99**, 210–219 (1955).
- [109] T. Fujii, T. Kondo, F. Takasaki, S. Yamada, S. Homma, K. Huke, S. Kato, H. Okuno, I. Endo, and H. Fujii, “Photoproduction of Charged π Mesons from Protons and Neutrons in the Energy Range Between 250 and 790 MeV,” *Nucl. Phys.* **B120**, 395–422 (1977).
- [110] G. Fischer, G. von Holtey, G. Knop, and J. Stumpfig, “Angular Distributions of Pions from $\gamma + p \rightarrow \pi^+ + n$ at Photon Energies between 220 and 425 MeV,” *Z. Phys.* **253**, 38–52 (1972); G. Fischer, H. Gischer, M. Heuel, G. von Holtey, G. Knop, and J. Stumpfig, “Photoproduction of Positive Pions on Hydrogen at Proton Energies Between 220 and 425 MeV,” *Nucl. Phys.* **B16**, 119–124 (1970).
- [111] C. Betourne, J. C. Bizot, J. Perez-Y-Jorba, and D. Treille, “Positive Pion Photoproduction from Hydrogen for Incident Photon Energies 300-750 MeV,” *Phys. Rev.* **172**, 1343–1354 (1968).
- [112] M. Beneventano, R. Finzi, L. Mezzetti, L. Paoluzi, and S. Tazzari, “Small-Angle Photoproduction of Single Positive Pions on Hydrogen at Energies Around the “Second Resonance,”” *Nuovo Cimento* **28**, 1464–1583 (1963).
- [113] F. P. Dixon and R. L. Walker, “Photoproduction of Single Positive Pions from Hydrogen in the 600- to 1000-MeV Region,” *Phys. Rev. Lett.* **1**, 458–460 (1958).
- [114] H.-W. Dannhausen, G. Fischer, H. M. Fischer, K. Kircher, M. Leneke, W. Niehaus, and H. Wessels, “Photoproduction of Positive Pions at 180° at Photon Energies from 0.4 to 1.4 GeV,” *Nucl. Phys.* **B61**, 285–295 (1973).
- [115] T. Fujii, H. Okuno, S. Orito, H. Sasaki, T. Nozaki, F. Takasaki, K. Takikawa, K. Amako, I. Endo, K. Yoshida, M. Higuchi, M. Sato, and Y. Sumi, “Charged- π Photoproduction at 180° in the Energy Range between 300 and 1200 MeV,” *Phys. Rev. Lett.* **26**, 1672–1675 (1971).
- [116] K. H. Althoff, G. Anton, B. Bock, D. Bour, W. Ferber, W. Ferber, H. W. Gelhausen, T. Jahnen, O. Kaul, D. Menze, W. Meyer, T. Miczaika, R. Müller, E. Roderburg, W. Ruhm, E. Schilling, W. J. Schulle, D. Sundermann, and K. Wagener, “Positive Pion Photoproduction from Hydrogen at Proton Energies Between 500 MeV and 1.400 MeV in Forward Direction,” *Z. Phys.* **C18**, 199–205 (1983).
- [117] S. D. Ecklund and R. L. Walker, “ π^+ Photoproduction from Hydrogen at Laboratory Energies from 589 to 1269 MeV,” *Phys. Rev.* **159**, 1195–1209 (1967).

- [118] R. A. Alvarez, G. Cooperstein, K. Kalata, R. C. Lanza, and D. Luckey, “Photoproduction of Positive Pions at Backward Angles in the Energy Range 1–3 GeV,” *Phys. Rev. D* **1**, 1946–1960 (1970); *Phys. Rev. Lett.* **21**, 1019–1022 (1968).
- [119] G. Buschhorn, J. Carroll, R. D. Eandi, P. Heide, R. Hübner, W. Kern, U. Kötz, P. Schmüser, and H. J. Skronn, “ π^+ Photoproduction Between 1.2 and 3 GeV at Very Small Angles,” *Phys. Rev. Lett.* **18**, 571–574 (1967).
- [120] L. Y. Zhu, J. Arrington, T. Averett *et al.*, “Cross-Section Measurement of Charged-Pion Photoproduction from Hydrogen and Deuterium,” *Phys. Rev. Lett.* **91**, 022003 (2003).
- [121] K. Ekstrand, A. Browman, L. Hand, and M. E. Nordberg, Jr., “Positive-Pion Photoproduction in the Backward Direction,” *Phys. Rev. D* **6**, 1–11 (1972).
- [122] V. K. Luk’yanov, V. A. Seliversov, and V. D. Toneev, “On the Pre-equilibrium Decay of Nuclei in Photonuclear Reactions,” *Yad. Fiz.* **21**, 992–1000 (1975) [*Sov. J. Nucl. Phys.* **21**, 508–512 (1975)].
- [123] K. K. Gudima, G. A. Ososkov, and V. D. Toneev, “Model for Pre-Equilibrium Decay of Excited Nuclei,” *Yad. Fiz.*, **21**, 260–272 (1975) [*Sov. J. Nucl. Phys.*, **21**, 138–143 (1975)].
- [124] S. G. Mashnik and V. D. Toneev, “MODEX—the Program for Calculation of the Energy Spectra of Particles Emitted in the Reactions of Pre-Equilibrium and Equilibrium Statistical Decays,” *JINR Communication P4-8417*, Dubna (1974).
- [125] A. G. Belov, Yu. P. Gangrskii, K. K. Gudima, and P. Zuzaan, “Integral Cross Sections of Photonuclear Reactions Near the Giant Resonance,” *Atomnaya Energiya*, **88**, 391–396 (2000) [*Atomic Energy*, **88**, 408–413 (2000)].
- [126] M. B. Chadwick, P. Oblizinsky, A. I. Blokhin, T. Fukahori, Y. Han, Y.-O. Lee, M. N. Martins, S. F. Mughabghab, V. V. Varlamov, B. Yu, and J. Zhang, *Handbook of Photonuclear Data for Applications: Cross Sections and Spectra*, IAEA-TECDOC-1178, IAEA, Vienna, October 2000, <http://www-nds-iaea.or.at/photonuclear/>; *IAEA Photonuclear Data Library. Cross Sections and Spectra up to 140 MeV*, LANL Report LA-UR-02-2002, LANL, Los Alamos, 20 January 2002, <http://t2.lanl.gov/data/photonuclear.html>.
- [127] Jürgen Ahrens, “The Total Absorption of Photons by Nuclei,” *Nucl. Phys.* **A446**, 229c–240c (1985); EXFOR File M0188.
- [128] G. R. Brookes, A. S. Clough, J. H. Freeland, W. Galbraith, A. F. King, T. A. Armstrong, W. R. Hogg, G. M. Lewis, A. W. Robertson, W. R. Rawlinson, N. R. S. Tait, J. C. Thompson, and D. W. L. Tolfree, “Total Hadronic Photoabsorption Cross Sections of Nuclei for Photons in the GeV Energy Range,” *Phys. Rev. D* **8**, 2826–2836 (1973); <http://www-spires.dur.ac.uk/cgi-bin/hepdata/testreac/1561/FULL/query>.
- [129] N. Bianchi, V. Muccifora, E. De Sanctis, A. Fantoni, P. Levi Sandri, E. Polli, A. R. Reolon, P. Rossi, M. Anghinolfi, P. Corvisiero, M. Ripani, M. Sanzone, M. Taiuti, and A. Zucchiatti, “Total Hadronic Photoabsorption Cross Section on Nuclei in the Nucleon Resonance Region,” *Phys. Rev. C* **54**, 1688–1699 (1996); EXFOR File M0590; <http://www-spires.dur.ac.uk/cgi-bin/hepdata/testreac/8767/FULL/query>.
- [130] N. A. Burgov, G. V. Danilyan, B. S. Dolbilkin, L. E. Lazareva, and F. A. Nikolaev, “Cross Section for Gamma-Absorption by Carbon in the Giant Resonance Region,” *Zh. Eksp. Teor. Fiz.* **45**, 1694–1703 (1963) [*Soviet Physics JETP* **18**, 1159–1166 (1964)]; EXFOR File M0160.002.
- [131] E. A. Arakelyan, G. L. Bayatyan, G. S. Vartanyan, N. K. Grigoryan, A. O. Kechechyan, S. G. Knyazyan, A. T. Margaryan, G. G. Marikyan, S. S. Stepanyan, and S. R. Shakhazizyan, “Measurement of the Total Cross Section for Photoproduction of Hadrons

- in Nuclei of Be, C, O, and Cu in the Range of Photon Energies $E_\gamma = 0.25\text{--}2.7$ GeV,” *Yad. Fiz.* **38**, 980–985 (1983) [*Sov. J. Nucl. Phys.* **38**, 589–592 (1983)]; <http://www-spires.dur.ac.uk/cgi-bin/hepdata/testreac/4684/FULL/query>.
- [132] E. A. Arakelyan, G. L. Bayatyan, G. S. Vartanyan, A. R. Voskanyan, N. K. Grigoryan, S. G. Knyazyan, A. T. Margaryan, G. G. Marikyan, S. S. Stepanyan, E. M. Oganessian, and S. R. Shakhazizyan, “Total Cross Sections for Photoproduction of π^0 Mesons and Hadrons in the Nuclei Be, C, O, and Al in the Energy Region $E_\gamma = 200\text{--}900$ MeV,” *Yad. Fiz.* **42**, 3–7 (1985) [*Sov. J. Nucl. Phys.* **41**, 1–3 (1985)]; <http://www-spires.dur.ac.uk/cgi-bin/hepdata/testreac/5366/FULL/query>.
- [133] V. Muccifora, N. Bianchi, A. Deppman, E. De Sanctis, M. Mirazita, E. Polli, and P. Rossi, “Photoabsorption on Nuclei in the Energy Range 0.5–2.6 GeV,” *Phys. Rev. C* **60**, 064616 (1999).
- [134] J. M. Wyckoff, B. Ziegler, H. W. Koch, and R. Uhlig, “Total Photonuclear Cross Sections for Low Atomic Number Elements,” *Phys. Rev.* **137**, B576–B592 (1965).
- [135] J. Ahrens, H. Borchert, K. H. Czock, H. B. Eppler, H. Gimm, H. Gundrum, M. Kröning, P. Riehn, G. Sita Ram, A. Zieger, and B. Ziegler, “Total Nuclear Photon Absorption Cross Sections for Some Light Elements,” *Nucl. Phys.* **A251**, 479–492 (1975); EXFOR File M0372.
- [136] J. Arends, J. Eyink, A. Hegerath, K. G. Hilger, B. Mecking, G. Nöldeke, and H. Rost, “Measurement of Total Photonuclear Cross Sections in the Δ -Resonance Region,” *Phys. Lett.* **B98**, 423–426 (1981).
- [137] S. Michalowski, D. Andrews, J. Eickmeyer, T. Gentile, N. Mistry, R. Talman, and K. Ueno, “Experimental Study of Nuclear Shadowing in Photoproduction,” *Phys. Rev. Lett.* **39**, 737–740 (1977); <http://www-spires.dur.ac.uk/cgi-bin/hepdata/testreac/2644/FULL/query>.
- [138] E. A. Arakelyan, G. L. Bayatyan, G. S. Vartanyan, N. K. Grigoryan, S. G. Knyazyan, A. T. Margaryan, S. S. Stepanyan, P. K. Kir’yanov, V. A. Maisheev, and A. M. Frolov, “Measurement of Total Hadronic Photoproduction Cross Section on the Nuclei C, Cu and Pb for Energies $E_\gamma = (12\text{--}30)$ GeV,” *Phys. Lett.* **B79**, 143–146 (1978); <http://www-spires.dur.ac.uk/cgi-bin/hepdata/testreac/2969/FULL/query>.
- [139] D. O. Caldwell, V. B. Elings, W. P. Hesse, R. J. Morrison, F. V. Murphy, and D. E. Young, “Total Hadronic Photoabsorption Cross Sections on Hydrogen and Complex Nuclei from 4 to 18 GeV,” *Phys. Rev. D* **7**, 1362–1383 (1973); <http://www-spires.dur.ac.uk/cgi-bin/hepdata/testreac/1559/FULL/query>.
- [140] A. Leprêtre, H. Beil, R. Bergère, P. Carlos, J. Fagot, A. De Miniac, and A. Veyssière, “Measurements of the Total Photonuclear Cross Sections from 30 MeV to 140 MeV for Sn, Ce, Ta, Pb, and U Nuclei,” *Nucl. Phys.* **A367**, 237–268 (1981).
- [141] S. C. Fultz, B. L. Berman, J. T. Caldwell, R. L. Bramblett, and M. A. Kelly, “Photoneutron Cross Sections for Sn^{116} , Sn^{118} , Sn^{119} , Sn^{120} , Sn^{124} , and Indium,” *Phys. Rev.* **186**, 1255–1270 (1969).
- [142] G. M. Gurevich, L. E. Lazareva, V. M. Mazur, S. Yu. Merkulov, G. V. Solodukhov, and V. A. Tyutin, “Total Nuclear Photoabsorption Cross Sections in the Region $150 < A < 190$,” *Nucl. Phys.* **A351**, 257–268 (1981); EXFOR File 90073.
- [143] O. A. P. Tavares, J. B. Martins, E. de Paiva, E. L. Moreira, J. L. Vieira, M. L. Terranova, M. Capogni, L. Casano, A. D’Angelo, D. Moricciani, F. Ghio, B. Girolami, and B. Babusci, “Fission Induced in ^{nat}Ta , ^{nat}W and ^{nat}Pt Targets by 69 MeV Monochromatic Photons,” *J. Phys. G* **19**, 805–811 (1993); EXFOR File M0380.

- [144] M. L. Terranova, O. A. P. Tavares, G. Ya. Kezerashvili, V. A. Kiselev, A. M. Milov, N. Yu. Muchnoi, A. I. Naumenkov, V. V. Petrov, I. Ya. Protopopov, E. A. Simonov, E. De Paiva, and E. L. Moreira, “Fissility of Bi, Pb, Au, Pt, W, Ta, V and Ti Nuclei Measured with 100 MeV Compton Backscattered Photons”, *J. Phys. G*, **22**, 511–522 (1996); EXFOR File M0390.
- [145] M. L. Terranova, G. Ya. Kezerashvili, A. M. Milov, S. I. Mishnev, N. Yu. Muchnoi, A. I. Naumenkov, I. Ya. Protopopov, E. A. Simonov, D. N. Shatilov, O. A. P. Tavares, E. De Paiva, and E. L. Moreira, “Photofission Cross Section and Fissility of Pre-Actinides and Intermediate-Mass Nuclei by 120 and 145 MeV Compton Backscattered Photons,” *J. Phys. G* **24**, 205–216 (1998); EXFOR File M0547.
- [146] J. B. Martins, E. L. Moreira, O. A. P. Tavares, J. L. Vieira, J. D. Pinheiro Filho, R. Bernabei, S. D’Angelo, M. P. de Pascale, C. Schaerf, and B. Girolami, “Nuclear Fission of ^{197}Au , ^{nat}Pb , and ^{209}Bi Induced by Polarized and Monochromatic Photons of 60 and 64 MeV,” *Nuovo Cimento* **A101**, 789–794 (1989); EXFOR File 90402.
- [147] J. B. Martins, E. L. Moreira, O. A. P. Tavares, J. L. Vieira, L. Casano, A. D’Angelo, C. Schaerf, M. L. Terranova, D. Babusci, and B. Girolami, “Absolute Photofission Cross Section of ^{197}Au , ^{nat}Pb , ^{209}Bi , ^{232}Th , ^{238}U , and ^{235}U Nuclei by 69-MeV Monochromatic and Polarized Photons”, *Phys. Rev. C* **44**, 354–364 (1991); EXFOR File M0388.
- [148] C. Chollet, J. Arends, H. Beil, R. Bergère, P. Bourgeois, P. Carlos, J. L. Fallou, J. Fagot, P. Garganne, A. Leprêtre, and A. Veyssière, “A Determination of the Total Photonuclear Absorption Cross Section for Pb in the Δ -Resonance Region by Means of a Neutron Multiplicity Measurement,” *Phys. Lett.* **B127**, 331–335 (1983); <http://www-spires.dur.ac.uk/cgi-bin/hepdata/testreac/4650/FULL/query>.
- [149] G. M. Gurevich, L. E. Lazareva, V. M. Mazur, G. V. Solodukhov, and B. A. Tulupov, “Giant Resonance in the Total Photoabsorption Cross Section of $Z \approx 90$ Nuclei,” *Nucl. Phys.* **A273**, 326–340 (1976); EXFOR File M0090.
- [150] Y. Birenbaum, R. Alarcon, S. D. Hoblit, R. M. Laszewski, and A. M. Nathan, “Photon Scattering on ^{238}U and the Interpretation of Near-Threshold Photofission Resonances,” *Phys. Rev. C* **36**, 1293–1297 (1987); EXFOR File 90263.
- [151] G. M. Gurevich, L. E. Lazareva, V. M. Mazur, and G. V. Solodukhov, “Total Cross Section for the Absorption of γ Quanta by Th^{232} , U^{235} , U^{238} , and Pu^{232} in the Region of Giant Dipole Resonance,” *Pis'ma Zh. Eksp. Teor. Fiz.* **20**, 741–745 (1974) [*JETP Letters*, **20**, 343–344 (1974)]; EXFOR File M0603.
- [152] N. K. Sherman, W. F. Davidson, A. Nowak, M. Kosaki, J. Roy, W. Delbianco, and G. Kajrys, “Electron-Pair Creation on the Uranium Nucleus,” *Phys. Rev. Lett.* **54**, 1649–1651 (1985); EXFOR File 90411.
- [153] O. A. P. Tavares, M. L. Terranova, L. Casano, A. D’Angelo, D. Moricciani, C. Schaerf, D. Babusci, B. Girolami, J. B. Martins, E. L. Moreira, and J. L. Vieira “Fission of Complex Nuclei Induced by 52-MeV Monochromatic and Polarized Photons,” *Phys. Rev. C* **44**, 1683–1686 (1991); EXFOR File M0387.
- [154] E. A. Arakelyan, A. R. Bagdsaryan, G. L. Bayatyan, G. S. Vartanyan, A. R. Voskanyan, N. KI. Grigoryan, S. G. Knyazyan, A. T. Margaryan, G. G. Marikyan, and A. K. Papyan, “Total Cross Section for Photoproduction of Hadrons in ^{235}U and ^{238}U in the Tagged Photon-Energy Region 0.3–3.5 GeV,” *Yad. Fiz.* **52**, 1387–1391 (1990) [*Sov. J. Nucl. Phys.* **52**, 878–880 (1990)].
- [155] N. Bianchi, A. Deppman, E. De Sanctis, A. Fantoni, P. Levi Sandri, V. Lucherini, V. Muccifora, M. Anghinolfi, P. Corvisiero, G. Gervino, L. Mazzaschi, V. Mokeev, G. Ricco, M. Ripani, M. Sanzone, M. Taiuti, A. Zucchiatti, R. Bergère, P. Carlos, P. Garganne, and A. Leprêtre, “Measurement of the Total Cross Section for ^{238}U Photofission in the Nucleon Resonance Region,” *Phys. Lett.* **B299**, 219–222 (1993).

- [156] *GEANT4 Physics Reference Manual*, <http://wwwasd.web.cern.ch/wwwasd/geant4/G4UsersDocuments/Overview/html/index.html>.
- [157] J. P. Wellisch, M. Kossov, and P. Degtyarenko, “Electro and Gamma Nuclear Physics in GEANT4,” paper **THMT004** in Proc. *Computing in High Energy and Nuclear Physics (CHEP03)*, La Jolla, California, March 24–28, 2003, <http://www.slac.stanford.edu/econf/C0303241>; E-print: nucl-th/0306012 (2003).
- [158] A. V. Prokofiev, S. G. Mashnik, and A. J. Sierk, “Cascade-Exciton Model Analysis of Nucleon-Induced Fission Cross Sections of Lead and Bismuth at Energies from 45 to 500 MeV,” *Nucl. Sci. Eng.* **131**, 78–95 (1999); E-print: nucl-th/9802027.
- [159] V. V. Varlamov, N. G. Efimkin, V. V. Surgutanov, A. A. Khoronenko, and A. P. Chernyaev, “Photonuclear Data. Photofission of Uranium U-235, 238,” Centre for Photonuclear Experimental Data [Centr Dannyykh Fotoyadernyykh Eksperimentov (CDFE)] Publication CDFE/FIS2, Moscow State University, 1987, EXFOR Data Base file M0300.003.
- [160] V. Lucherini, C. Guaraldo, E. De Sanctis, P. Levi Sandri, E. Poli, A. R. Reolon, A. S. Iljinov, S. Lo Nigro, S. Aiello, V. Bellini, V. Emma, C. Milone, G. S. Pappalardo, and M. V. Mebel, “Au Photofission Cross Section by Quasimonochromatic Photons in the Intermediate Energy Region,” *Phys. Rev. C* **39**, 911–916 (1989).
- [161] G. Andersson, I. Blomqvist, B. Forkman, G. G. Jonsson, A. Järund, K. Kroon, K. Lindgren, B. Schroder, and K. Tesh, “Photon-Induced Nuclear Reactions above 1 GeV. (I) Experiment,” *Nucl. Phys.* **A197**, 44–70 (1972).
- [162] M. L. Terranova, A. D’Angelo, J.D. Pinheiro, E. S. De Alme, E. Z. Bilbao, and J. B. Martins, “Fission Yields of ^{209}Bi and ^{nat}Pb Nuclei Induced by Photon Beams of 226 MeV Maximum Energy from Compton Backscattered Laser Light,” *Nuovo Cimento* **A105**, 197–202 (1992); EXFOR File M0502.
- [163] C. Cetina, P. Heimberg, B. L. Berman, W. J. Briscoe, G. Feldman, L. Y. Murthy, Hall Crannell, A. Longhi, D. I. Sober, J. C. Sanabria, and G. Ya. Kezerashvili, “Photofission of Heavy Nuclei from 0.2 to 3.8 GeV,” *Phys. Rev. C* **65**, 044622 (2002).
- [164] H.-D. Lemke, B. Ziegler, M. Mutterer, J. P. Theobald, N. Cârjan, “Absolute Photofission Cross Section of ^{209}Bi in the Energy Range from 40 to 65 MeV,” *Nucl. Phys.* **A342**, 37–52 (1980); EXFOR File M0587.
- [165] V. Bellini, V. Emma, S. Lo Nigro, C. Milone, G. S. Pappalardo, E. De Sanctis, P. Di Giacomo, C. Guaraldo, V. Lucherini, E. Polli, and A. R. Reolon, “Fission of Bi Induced by a Quasi-Monochromatic Photon Beam at Energies from 100 MeV to 280 MeV,” *Lett. Nuovo Cimento* **36**, 587–592 (1983).
- [166] L. G. Moretto, R. C. Gatti, S. G. Thompson, J. T. Routti, J. H. Heisenberg, L. M. Middleman, M. R. Yearian, and R. Hofstadter, “Electron- and Bremsstrahlung-Induced Fission of Heavy and Medium-Heavy Nuclei,” *Phys. Rev.* **179**, 1176–1187 (1969).
- [167] E. V. Minarik and V. A. Novikov, “Fission of U, Th, Bi and Tl Induced by High Energy γ -Quanta,” *Zh. Eksp. Teor. Fiz.* **32**, 241–246 (1957) [*Sov. Phys. JEPT* **5**, 253–257 (1957)].
- [168] M. L. Terranova, G. Ya. Kezerashvili, V. A. Kiselev, A. M. Milov, S. I. Mishnev, I. Ya. Protopopov, V. N. Rotaev, D. N. Shatilov, and O. A. P. Tavares, “Fission Cross Section and Fissility of ^{209}Bi by 60–270 MeV Tagged Photons,” *J. Phys. G*, **22**, 1661–1672 (1996).
- [169] Yu. N. Ranyuk and P. V. Sorokin, “Photofission of Bi, Pb, Au, Pt, Os, Re, Ta, and Hf below 260 MeV,” *Yad. Fiz.* **5**, 37–41 (1967) [*Sov. J. Nucl. Phys.* **5**, 26–29 (1967)].

- [170] C. Guaraldo, V. Lucherini, E. De Sanctis, P. Levi Sandri, E. Polli, A. R. Reolon, S. Lo Nigro, S. Aiello, V. Bellini, V. Emma, C. Milone, and G. S. Pappalardo, “Photoexcitation Mechanisms and Photofission Cross Section for Bi by 100–300 MeV Quasi-Monoenergetic Photons,” *Phys. Rev. C* **36**, 1027–1036 (1987).
- [171] John A. Jungerman and Herbert M. Steiner, “Photofission Cross Sections of U^{235} , U^{236} , U^{238} , Th^{232} , Bi^{209} , and Au^{197} at Energies of 150 to 500 MeV,” *Phys. Rev.* **106**, 585–590 (1957).
- [172] J. T. Caldwell, E. J. Dowdy, B. L. Berman, R. A. Alvarez, and P. Meyer, “Giant Resonance for the Actinide Nuclei: Photoneutron and Photofission Cross Sections for ^{235}U , ^{236}U , ^{238}U , and ^{232}Th ,” *Phys. Rev. C* **21**, 1215–1231 (1980).
- [173] S. P. Kapitza, N. S. Rabotnov, G. N. Smirenkin, A. S. Soldatov, L. N. Usachev, and Yu. M. Tsipenyuk, “Photofission of Even-Even Nuclei and Structure of Fission Barrier,” *Pis'ma Zh. Eksp. Teor. Fiz.* **9**, 128–132 (1969) [*JETP Letters* **9**, 73–76 (1969)].
- [174] A. Leprêtre, R. Bergère, P. Bourgeois, P. Calos, J. Fagot, J. L. Fallou, P. Garganne, A. Veyssière, H. Ries, R. Göbel, U. Kneissl, G. Mank, H. Ströher, W. Wilke, D. Ryckbosch, and J. Jury, “Absolute Photofission Cross Sections for ^{232}Th and $^{235,238}U$ Measured with Monochromatic Tagged Photons ($20\text{ MeV} < E_\gamma < 110\text{ MeV}$),” *Nucl. Phys.* **A472**, 533–557 (1987).
- [175] A. Veyssière, H. Beil, R. Bergère, P. Carlos, A. Lepretre, “A Study of the Photofission and Photoneutron Processes in the Giant Dipole Resonance of ^{232}Th , ^{238}U and ^{237}Np ,” *Nucl. Phys.* **A199**, 45–64 (1973).
- [176] H. X. Zhang, T. R. Yeh, and H. Lancman, “Photofission Cross Section of ^{232}Th ,” *Phys. Rev. C* **34**, 1397–1405 (1986).
- [177] B. L. Berman, J. T. Caldwell, E. J. Dowdy, F. S. Dietrich, P. Meyer, and R. A. Alvarez, “Photofission and Photoneutron Cross Sections and Photofission Neutron Multiplicities for ^{233}U , ^{234}U , ^{237}Np , and ^{239}Pu ,” *Phys. Rev. C* **34**, 2201–2214 (1986); EXFOR File L0058.002.
- [178] M. A. P. V. de Moraes and M. F. Cesar, “Photonuclear Cross Sections of ^{233}U Using Neutron Capture Gamma Rays Near Threshold,” *Nuovo Cimento* **A106**, 1165–1173 (1993); EXFOR File M0381.002.
- [179] J. R. Huizenga, K. M. Clarke, J. E. Gindler, and R. Vandenbosch, “Photofission Cross Sections of Several Nuclei with Mono-Energetic Gamma Rays,” *Nucl. Phys.* **34**, 439–456 (1962); EXFOR File M0505.007.
- [180] Yu. B. Ostapenko, G. N. Smirenkin, A. S. Soldatov, V. E. Zhuchko, and Yu. M. Tsipenyuk, “Yields and Cross Sections of Photofission for Isotopes Th, U, Np, and Am in Energy Range from 4.5 MeV to 7.0 MeV,” *Voprosy Atomnoy Nauki i Tekhniki, Seriya Yadernye Konstanty* **3(30)**, 3 (1978); [in Russian]; EXFOR Files M0004.005 and M0004.013.
- [181] H. Ries, U. Kneissl, G. Mank, H. Ströher, W. Wilke, R. Bergère, P. Bourgeois, P. Carlos, J. L. Fallou, P. Garganne, A. Veyssière, and L. S. Cardman, “Absolute Photofission Cross Sections of $^{235,238}U$ Measured with Tagged Photons between 40 and 105 MeV,” *Phys. Lett.* **B139**, 254–258 (1984); EXFOR File M0492.003.
- [182] Th. Frommhold, F. Steiper, W. Henkel, U. Kneissl, J. Ahrens, R. Beck, J. Peise, M. Schmitz, I. Anthony, J. D. Kellie, S. J. Hall, and G. J. Miller, “Photofission of ^{235}U and ^{238}U at Intermediate Energies: Absolute Cross Sections and Fragment Mass Distributions,” *Z. Phys.* **A350**, 249–261 (1994).
- [183] W. Cesar Khouri, Final Report to the IAEA on the Research Contract NDT-18, sent to the IAEA on May 10, 1983; EXFOR File G0002.003.

- [184] A. S. Soldatov, “Photofission Cross Section of Uranium-234 in the Energy Region from 5 to 9 MeV and Its Comparison with the Data for Thorium-232 and Neptunium-237 in Subbarrier Region,” *Voprosy Atomnoy Nauki i Tekhniki, Seriya Yadernye Konstanty* **1-2**, 8 (1997) [in Russian]; EXFOR File M0544.007.
- [185] S. G. Mashnik, K. K. Gudima, I. V. Moskalenko, R. E. Prael, and A. J. Sierk, “CEM2k and LAQGSM Codes as Event Generators for Space-Radiation-Shielding and Cosmic-Ray-Propagation Applications,” *Adv. Space Res.* **34**, 1288–1296 (2004).
- [186] V. D. Toneev and K. K. Gudima, “Particle Emission in Light and Heavy-Ion Reactions,” *Nucl. Phys.* **A400**, 173c–190c (1983).
- [187] R. A. Schumacher, G. S. Adams, D. R. Ingham, J. L. Matthews, W. W. Sapp, R. S. Turley, R. O. Owens, and B. L. Roberts, “Cu(γ, p)X Reaction at $E_\gamma = 150$ and 300 MeV,” *Phys. Rev. C* **25**, 2269–2277 (1982); EXFOR File M0586.
- [188] M. Anghinolfi, V. Lucherini, N. Bianchi, G. P. Capitani, P. Corvisiero, E. De Sanctis, P. Di Giacomo, C. Guaraldo, P. Levi-Sandri, E. Polli, A. R. Reolon, G. Ricco, M. Sanzone, and M. Taiuti, “Inclusive Photoproton Spectra from ^{12}C at Intermediate Energies,” *Nucl. Phys.* **A457**, 645–656 (1986).
- [189] K. G. Fissum, H. S. Caplan, E. L. Kallin, D. M. Skopik, J. M. Vogt, M. Frodyma, D. P. Rosenzweig, D. W. Storm, G. V. O’Rielly, and K. R. Garrow, “Inclusive Positive Pion Photo-production,” *Phys. Rev. C* **53**, 1278–1289 (1996).
- [190] L. I. Schiff, “Energy-Angle Distribution of Thin Target Bremsstrahlung,” *Phys. Rev.* **83**, 252–253 (1951).
- [191] D. N. Olson, Ph.D. thesis, Cornell University, 1960.
- [192] D. H. Boal and R. M. Woloshin, “Role of Direct Emission in Strong and Electromagnetically Induced Inclusive Reactions,” *Phys. Rev. C* **23**, 1206–1216 (1981).
- [193] J. L. Matthews and W. Turchinets, LNS Internal Report No. 110, 1966.
- [194] S. Kabe, S. Kato, T. Kifune, Y. Kimura, M. Kobayashi, K. Kondo, Y. Nagashima, and T. Nishikawa, “Photoproduction of Positive Pions from Carbon Nuclei,” *J. Phys. Soc. Japan* **19**, 1800–1808 (1964).
- [195] Koh Sakamoto, “Radiochemical Study on Photonuclear Reactions of Complex Nuclei at Intermediate Energies,” *J. Nucl. Radiochem. Sci.* **4**, A9–A31 (2003).
- [196] Hiromitsu Haba, “Recoil Studies of Photonuclear Reactions at Intermediate Energies,” *J. Nucl. Radiochem. Sci.* **3**, A11–A20 (2002).
- [197] T. A. Gabriel and R. G. Alsmiller, Jr., “Photonuclear Disintegration at High Energies (< 350 MeV),” *Phys. Rev.* **182**, 1035–1050 (1969).
- [198] T. A. Gabriel, M. P. Guthrie, and O. W. Hermann, “Instructions for the Operation of the Program PICA, an Intra-Nuclear Cascade Calculation for High Energy (30–400 MeV) Photon-Induced Nuclear Reactions,” Oak Ridge National Laboratory Report ORNL-4687 (1971).
- [199] C. Y. Fu, T. A. Gabriel, and R. A. Lille, “PICA95: An Intranuclear-Cascade Code for 25 MeV to 3.5 GeV Photon-Induced Nuclear Reactions,” *Proc. SATIF-3, Sendai, Japan, 12–13 May, 1997*, NEA/OECD, Paris, France, 1998, pp. 49–60.
- [200] Tatsuhico Sato, Kazuo Shin, Syuichi Ban, Yoshihito Namito, Hajime Nakamura, and Hideo Hirayama, “Modification of Photo-Nuclear Cascade Evaporation Code PICA95 at Energies Below 150 MeV,” *Nucl. Instr. Meth.* **A437**, 471–480 (1999).
- [201] T. Sato, K. Shin, S. Ban, T. A. Gabriel, C. Y. Fu, and H. S. Lee, “PICA3, An Update Code of Photo-nuclear Cascade Evaporation Code PICA95, and its Benchmark Experiments,” *Proc. MC2000, Lisbon, Portugal, October 23–26, 2000*,

- [202] H. Haba, M. Igarashi, K. Washiyama, H. Matsumura, M. Yamashita, K. Sakamoto, Y. Oura, S. Shibata, M. Furukawa, and I. Fujiwara, “Photofission of ^{197}Au at Intermediate Energies,” *J. Nucl. Radiochem. Sci.* **1**, 53–61 (2000).
- [203] H. Haba, M. Kasaoka, M. Igarashi, K. Washiyama, H. Matsumura, Y. Oura, S. Shibata, K. Sakamoto, M. Furukawa, and I. Fujiwara, “Photofission of ^{209}Bi at Intermediate Energies,” *Radiochim. Acta* **90**, 371–382 (2002).
- [204] T. Methasiri and S. A. E. Johansson, “High-Energy Photofission of Heavy and Medium-Heavy Elements,” *Nucl. Phys.* **A167**, 97–107 (1971).
- [205] I. Kroon and B. Forkman, “Intermediate Energy Photofission in Tantalum, Gold and Lead,” *Nucl. Phys.* **A179**, 141–152 (1972).
- [206] P. David, J. Debrus, U. Kim, G. Kumbartzki, H. Mommsen, W. Soye, K. H. Speidel, and G. Stein, “High-Energy Photofission of Gold and Uranium,” *Nucl. Phys.* **A197**, 163–176 (1972).
- [207] G. A. Vartapetyan, N. A. Demekhina, V. I. Kasilov, Yu. N. Ranyuk, P. V. Sorokin, and A. G. Khudaverdyan, “Photofission Cross Sections Up to 5 BeV: Supergiant Resonance in Photonuclear Reactions,” *Yad. Fiz.* **14**, 65–72 (1971) [*Sov. J. Nucl. Phys.* **14**, 37–40 (1972)].
- [208] V. Emma, S. Lo Nigro, and C. Milone, “Fission Yields of 28 Elements by Bremsstrahlung Photons of 1000 MeV Maximum Energy,” *Nucl. Phys.* **A257**, 438–444 (1976).
- [209] F. M. Kiely and B. D. Pate, “Study by Track Detectors of the 580-MeV Photofission of U, Au, Te, Ag, Cu and Cr,” *Z. Physik* **A279**, 331–338 (1976).
- [210] G. Bernardini, R. Reitz, and E. Segre, “Photomesonic Fission of Bismuth,” *Phys. Rev.* **90**, 573–574 (1953).
- [211] H. G. de Carvalho, G. Cortini, E. del Giudice, G. Potenza, R. Rinzivillo, and G. Ghigo, “Photofission of Bi, W and Ag from 300 to 1000 MeV,” *Nuovo Cimento* **32**, 293–297 (1964).
- [212] H. G. de Carvalho, J. B. Martins, O. A. Tavares, V. di Napoli, M. L. Teranova, and K. Tesch, “Photofission Cross-Sections of ^{209}Bi , ^{232}Th , and ^{238}U Above 1 GeV,” *Lett. Nuovo Cimento*, **14**, 615–297 (1975).
- [213] Koh Sakamoto, Samir Ranjan Sarkar, Yasuji Oura, Hiromitsu Haba, Hiroshi Matsumura, Yutaka Miyamoto, Seiichi Shibata, Michiaki Furukawa, and Ichiro Fujiwara, “Mass Yield Feature of (γ, π^+) and (γ, π^-n) Reactions for $x = 0-9$ on Complex Nuclei in the Δ Region,” *Phys. Rev. C* **59**, 1497–1505 (1999).
- [214] S. R. Sarkar, M. Soto, Y. Kubota, M. Yoshida, T. Fukasawa, K. Matsumoto, K. Kawaguchi, K. Sakamoto, S. Shibata, M. Furukawa, and I. Fujiwara, “Photospallation of Complex Nuclei at Intermediate Energies. I,” *Radiochim. Acta* **55**, 113–137 (1991).
- [215] Hiroshi Matsumura, Koshin Washiyama, Hiromitsu Haba, Yutaka Miyamoto, Yasuji Oura, Koh Sakamoto, Seiichi Shibata, Michiaki Furukawa, Ichiro Fujiwara, Hisao Nagai, Takayuki Kobayashi, and Koichi Kobayashi, “Target-Dependence of Light Fragment Production in Photonuclear Reactions at Intermediate Energies,” *Radiochim. Acta* **88**, 313–328 (2000).
- [216] M. Yamashita, K. Yoshida, Y. Terada, A. Nagano, Y. Kawashima, D. Osada, H. Matsumura, K. Washiyama, K. Sakamoto, Y. Miyamoto, Y. Oura, S. Shibata, I. Fujiwara, and M. Furukawa, *Proc. 43rd Symp. on Radiochemistry*, Oct. 13–15, 1999, Tsukuba, Japan, *Suppl. to J. Nucl. Radiochem. Sci.* **1** (1999) Abstract 3P17.
- [217] Yu. E. Titarenko, O. V. Shvedov, V. F. Batyaev, E. I. Karpikhin, V. M. Zhivun, A. B. Koldobsky, R. D. Mulambetov, S. V. Kvasova, A. N. Sosnin, S. G. Mashnik, R. E. Prael, A. J. Sierk, T. A. Gabriel, M. Saito, and H. Yasuda, “Cross Sections for Nuclide Production in 1 GeV Proton-Irradiated ^{208}Pb ,” *Phys. Rev. C* **65**, 064610 (2002).

- [218] D. Ryckbosch, L. Van Hoorebeke, R. Van de Vyver, F. De Smet, J-O. Adler, D. Nilsson, B. Schröder, and R. Zorro, “Determination of the Absorption Mechanism in Photon-Induced Pre-Equilibrium Reactions,” *Phys. Rev. C* **42**, 444–447 (1990).